Material properties data for heat transfer modeling in Nb_3Sn magnets

Andrew Davies

Abstract

A Network Model is used to study the thermal behavior of magnet coils and to calculate the quench levels of the superconducting magnets. The cryogenic materials properties data are essential input for heat transfer calculation in superconducting magnets. In order to prepare this input and to study of model sensitivity on different material properties parameterizations a material data compilation is required. The collected data will be implemented into thermal magnet model to calculate the thermal behavior of superconducting magnets as well as to assess the magnet components crucial to heat transfer in the magnet.

1. Introduction

The accelerator superconducting magnets quench, especially in Large Hadron Collider (LHC) [1], is undesirable. In order to minimize the number of quenches, one needs to calculate the quench limit of each proposed magnet design.

This paper is focusing on material properties data required for thermal modeling of superconducting magnets, particularly on available material data at low temperatures as well as heat transfer in solid materials. The measured material properties in the

temperature range 1-300 K were collected and organized. The compiled dataset will be used inter alia as input to the thermal model of Nb_3Sn superconducting magnets.

1.1 Heat conductivity

Thermal conductivity is the property of a material's ability to conduct heat. Thermal conductivity in a steady state, unidirectional heat flow through an isotropic medium can be defined by the Fourier-Biot equation

$$\frac{\dot{Q}}{A} = -k\frac{dT}{dx} \qquad \text{Eq. 1}$$

Where $\dot{Q}$ [J] is rate of heat flow through area A [m^2] with a temperature gradient, dT/dx [K/m] and k [W/mK] is thermal conductivity.

In order to get the total heat conductivity additional terms with linear temperature dependence can be added to Eq. 1. In metals and dilute alloys heat conductivity is dominated by free electrons. More highly alloyed metals have decreased free electron heat conductivity and in this case the phonons heat conduction dominates. In semiconducting materials electron-hole pair conduction contributes to the electron and phonon components. Phonons conduction is the primary heat transfer mechanism in all other non-metallic materials. Thermal conductivity is temperature dependent, in general decreases as the temperature is lowered.

At low temperatures the generic name, e.g. copper, titanium, carbon, of a material is generally not sufficient to characterize the thermal conductivity. This is because sample variables such as lattice imperfections, impurities, magnetic fields, size of sample, and shape of sample can all effect thermal conductivity by orders of magnitude. It is vital to pick the “best value” of a material of for a specific application. A good overview of thermal conductivity is given by Reed and Clark in [44].

1.2 Heat capacity

Heat capacity is defined as the amount of heat required to raise the temperature of a system by a unit of temperature. The SI unit of heat capacity is the J/K. It is defined as:

$$C = -\left(\frac{dq}{dT}\right)_x \qquad \text{Eq. 2}$$

where q [J] is heat, T [K] is temperature, and x can be either volume or pressure.

Heat capacity is an extensive property, particular to the samples. It is useful to present heat capacity as an intensive variable, making it intrinsic characteristic of a particular substance, rather than sample dependent. In this case it is known as specific heat capacity. Specific heat is the heat capacity per unit mass of a material, [J/kg K]. Also molar heat capacity [J/mol K] or volumetric-specific heat capacity heat, [J/m^3 K]

are commonly used. In a gas molar heat capacity is more useful when in a solid either specific or volumetric-heat capacity is used, depending on the known information.

Specific heat is a strong function of temperature as can be seen in the experimental graphs in the Appendix. The experimental data show that below 100 K specific heat approximately decreases as T^3 in most materials. At very low temperatures, below 10 K specific heat becomes linear and according to the third law of thermodynamics it goes to zero at 0 K. For temperatures above 100 K specific heat typically approaches a constant value [44].

The value of specific heats of most materials at room temperature is of order of 25 [J/mol K]. This number is known as the Dulong-Petit value [44]. This value holds well for elements that lack strong inter-atomic forces. Boltzmann justified this theoretically with the equipartition-of-energy theorem [44]. Equipartition theory states that in thermal equilibrium energy is shared equally among the degrees of freedom. In a solid, there are six degrees of freedom associated with lattice vibrations. Quantum effects become significant at low temperatures, resulting in equipartition-of-energy theorem to overestimate specific heat. This is because the difference between quantum energy levels in a degree of freedom exceeds the average thermal energy of the system. In this case, the degree of freedom is said to be frozen out. The result is that the degree of freedom cannot store thermal energy and can no longer contribute to the specific heat.

Einstein was the first to apply quantum concepts to the thermal vibrations of atoms and molecules in a solid crystal lattice. The quantized thermal vibrations have become known as phonons. He assumed that particles of a crystal lattice oscillated independently of one another at a single frequency. This theory works well for high temperatures but fails in the low temperature range. The problem with Einstein's theory was the assumption of a single allowable frequency of vibration [44].

Debye treated a crystalline solid as an infinite elastic continuum and visualized the excitement of all the possible elastic standing waves in the material [44]. Debye also established a lower limit to the wavelengths that could exist in the crystal. Phonons are the chief means of storing energy in solids and thus dominate the heat capacity of most materials in cryogenic temperature range. The phonon contribution to the specific heat at constant volume C_v may be estimated by the Debye function.

$$C_V = 9rR\left(\frac{T}{\theta_D}\right)^3 \int_0^{X_{max}} e^x \cdot \frac{X^4}{(e^X-1)\text{^}2} dX \qquad \text{Eq. 3}$$

At high temperatures ($\theta_d/T<0.1$) this may be approximated by

$$C_v = 3rR\left(1 - \frac{X^2}{20} + \frac{X^4}{560} - \frac{X^6}{18144}\right) \qquad \text{Eq. 4}$$

Where $X=h\nu/kT$, $X_{max}=h\nu_{max}/kT$, and r = number of atoms per molecule. At low temperatures ($T< \theta_d/10$ K), it may be approximated by

$$C_v = 1944r\left(\frac{T}{\theta_d}\right)^3 \frac{J}{mol\cdot K} = \beta T^3 \qquad \text{Eq. 5}$$

However at low temperatures the electronic contribution to specific heat becomes significant [44]. This term can be added to the Debye model to give the total specific heat at low temperatures.

$$C = \beta T^3 + \gamma T \qquad \text{Eq. 3}$$

For ferromagnetic and ferrimagnetic materials a term δT^(3/2) would also contribute [44]. For antiferromagnetic materials a term ξT^3 would contribute, however it is difficult to differentiate this term form the phonon contribution. This approximation works well up to 80 K for most metals. [44]

The agreement between Debye theory and experimental results is remarkably good for many solids, specifically at $T < \theta_d = h\nu_{max}/k$ (θ_d -Debye characteristic temperature). [45] Debey temperatures typically are between 100 and 400 K, such as Niobium with a body center cubic structure has a θ_d = 250 K. [43] Though some materials are can have much higher Debye temperatures such as diamond with a Debye temperature of 2000 K. [43] It also recovers the Dulong-Petit law at high temperatures [44]. However at intermediate temperatures if suffers from inaccuracies due to theoretical simplifications. Debye's theory was enhanced by Born, Blackman and Karman [45] who considered inter-atomic forces and calculated the frequency spectrums of the lattice vibrations in more detail.

1.3 Guide to this database

Typically Cp is measured experimentally and C_v is derived theoretically, see reference [44] for full details. It is useful to note that the difference between C_p and C_v at low temperatures is quite small. It is usually ~1% at temperatures near $\theta_D/2$. [43] So for most purposes, we can use the two interchangeably at cryogenic temperatures.

Data is shown as tables, equations, and graphs. Analytical equations have been provided when possible. The objective was to provide a reliable equation for all materials across the full cryogenic temperature range. Graphs and figures comparing different data sets are presented in the appendix.

Data is organized into insulators, superconductors, and metals chapters. Every data set is labeled with a number in brackets that corresponds to a reference. Reference can be found in the bibliography. Equations are labeled with temperature and magnetic ranges that they are applicable. When available, uncertainty is kept with the raw data, in tabulated form. If uncertainty analysis is unavailable it must be implied form significant digits. Certain materials have special parameters that greatly affect their properties. Details in these cases are given below.

This database is not exhaustive. It does give information on the validity of different datasets. Certain materials require particular attention to the specific circumstances, often time cause large variations between samples of the same materials. Other materials have simple behavior and there is good agreement between measurements.

2 Material properties

2.1 Insulation: G10

G10 insulation is commonly used in prototypes of Nb_3Sn accelerator magnets. A name of G10 is used for composition consisting of epoxy (resin) and fiberglass. G-10 is a loose definition of fiberglass and resin and does not describe a particular material; it is a NEMA specification describing electrical and mechanical properties [50]. The actual composition is not well defined. G-10's thermodynamic properties will change for different manufactures. G-10's poperties should be a function of the fiberglass resin ratio. Studies by Imbasciati [30] have made attempts to estimate this ratio. G-10 CR is specifically designed for cryogenic applications. G-10CR's thermodynamic properties are consistent [50]. The data in figures ? and ? confirm this.

2.1.1 Specific heat of G10

G10 data for the specific heat is summarized in figures ? and ?. Due to the limited sources of data on G10, data was also gathered on related materials of epoxies and glass. It is suspect that G10 should have a specific heat capacity between glass and the epoxy. Fermilab uses CTD-101K Epoxy and S-2 glass for the Nb_3Sn based magnets. The G10 is also painted with a ceramic binder (CTD 1008x) applied on the coils after winding.

Specific heat data could not be found on CTD-101K. Data on other epoxy was gathered but shown considerable variation between brands. From figure ?, it can be seen that glass has a lower specific heat then all G-10 data at all but one epoxy dataset.

The only study that could be found on the ceramic binder was done by Imbasciati [30]. However this study was done with ceramic fibers rather the glass fibers.

Reference [13] G-10 CR

$$C = 10^{-2.4083+7.6006\cdot x-8.2982\cdot x^2+7.3301\cdot x^3-4.2386\cdot x^4+1.4294\cdot x^5-.24396\cdot x^6+.015236\cdot x^7}\ \frac{J}{kg\cdot K}$$

Where $x = \log_{10}(T)$, valid for $1<T<300$ K, equation has a 2% error from data and it is extrapolated below 4 K. Comparison to other data below 4K shows good agreement, justifying the extrapolation.

2.1.2 Heat conductivity of G10

This is the largest uncertainty of all material properties. This can not be estimated from epoxy and glass material properties [30] just as in the cause of specific heat G-10 CR is consistent between datasets while G-10 is divergent. In addition a factor of the ceramic binder CTD-1002X affecting the G-10 thermal conductivity. There is no experimental data on CTD-1002X in G10. It effects remain unknown. Though G10

thermal conductivity remains below .3 W/(m*K) under 20 K for all data. According to [33] the conductivity is strongly depended on the treatment of the glass mica tape.

Experiments from [33] show that it can vary by a factor of 4 at 4 K from treatment processes alone.

G10's thermal conductivity is directional in the cable, thus typically two values are given. The normal direction is of most interested for modeling of superconducting magnets.

Reference [22]

$$k = 0.0179T - 0.0129$$

From 0 K to 4 K the data was extrapolated. The values were computed by a computer program "MATPRO" the accuracy of these values is within an error of about 10%-20%.

Reference: G-10CR(Normal) tabulated data from [43] was fitted to the following equations

$$k = -3.622999163833060E\text{-}14x^6 + 2.996579202182310E\text{-}11x^5 - 9.687545615732300E\text{-}09x^4 + 1.599284085411630E\text{-}06x^3 - 1.452811767382280E\text{-}04x2 + 8.279441504868440E\text{-}03x + 4.082144325604080E\text{-}02$$

Valid for $4<T<150$ K, $R^2 = 9.999974932079730E\text{-}01$

Reference: G-10 CR Norm [13]

$$k=10^{(-4.1236+13.788*Log(T)-26.068*Log(T)^2+26.272*Log(T)^3-14.663*Log(T)^4+4.4954*Log(T)^5-0.6905*Log^6+0.0397*Log(T)^7)}$$

Valid for 10<T<300 K

2.2 Insulation – Polyimide

There are number of brands of Polyimide, LARP magnets use the brand kapton, polypyromellitimide (PPMI). [51] There are a number of different grades of kapton.

2.2.1 Specific heat of Polyimide

There is limited data on polyimide heat capacity. Kapton heat capacity data diverges at low temperatures. It could be due to different grades of kapton failing to be reported.

References: Kapton *[13], [25], [51]*

C =10^(-1.3684+.65892x+2.8719x^2+.42651x^3-3.0088x^4+1.9558x^5-.51998x^6+.051574x^7)

Where $x = \log_{10}(T)$

Valid for 4<T<300 K, curve fit 3 % error relative to data

2.2.2 Heat conductivity of Polyimide

Kapton of different grades have different thermal conductivities. [28] Few sources reported there grade of kapton. Most likely the grade was HN regular kapton.

References: Tabulated data from [13][25][40] was fitted to the following equations

$$k = -5.549425651993340E\text{-}08x^6 + 3.218098410811410E\text{-}06x^5 - 7.308479874262390E\text{-}05x^4 + 8.081548087134060E\text{-}04x^3 - 4.310834101394770E\text{-}03x^2 + 1.124627001832080E\text{-}02x - 1.460019416713240E\text{-}03$$

Valid for 1.9<T<15K, $R^2 = 9.998980502202240E\text{-}01$

References [13][25][51]

k=10^(5.73101-39.5199(logT)+79.9313(logT)^2-83.8572(logT)^3+50.9157(logT)^4-17.9835(logT)^5+3.42413(logT)^6-.27133(logT)^7 (W/(m*K))

Valid for 4<T<300k

Reference [28]

k=5.24+/-.32*10^(-3)T^(1.02+/-.02) (W/(m*K))

Valid in 5<T<300 K. This data is higher than all other datasets. However it is a different makeup then HN regular kapton. It matches kapton H films well.

2.3 Superconductors and alloys - NbTi

2.3.1 Specific heat of NbTi

Niobium Titanium specific heat data exhibits the characteristic second order phase transition peak, figure ?. This peak shifts to the left with increasing magnetic field. Specific heat data diverges at higher temperature. This is likely due to different alloy compositions. Few sources reported information on elemental %.

Reference [17] dataset 3

$$C_{pNC}=.0023*T^3+.145*T \text{ (J/(kg*K))}$$

Valid for 4.2<T<20 K

$$C_{pSC}=(.0023+3*.145/(9.1^2))*T^3+(.145*B/14)*T \text{ (J/(kg*K))}$$

Valid for T<9.1 K, 0<H<7 T

Reference [25]

$$C_{NC}=.1546667*T+.002706667*T^3 \text{ (J/(kg*K))}$$

Valid for Tc<T<20 K, assuming density (kg/m^3)=6000

$$C_{NC}=.165714286*T+.0029*T^3 \text{ (J/(kg*K))}$$

Valid for Tc<T<20 K, assuming density (kg/m^3)=5600

$$C_{NC} =6.9-1.307683333*T+0.092285*T^2+1.996666667*10^(-3)*T^3-3.633333333*10^(-5)*T^4 \text{ (J/(kg*K))}$$

Valid for 20<T<50 K density (kg/m^3)=6000

$$C_{NC} =7.392857143-1.401089286*T+0.098876786*T^2+0.002139286*T^3-0.000038929*T^4$$

Valid for 20<T<50 K density (kg/m^3)=5600

$$C_{NC} =-255+13.837*T-.119383333*T^2+.000496*T^3-8.03333\times 10^(-7)*T^4 \text{ (J/(kg*K))}$$

Valid for 50<T<175 K density (kg/m^3)=6000

$$C_{NC} =-273.2142857 +14.82535714*T-.127910714*T^2+.000531429*T^3-8.607142857*10^(-7)*T^4 \text{ (J/(kg*K))}$$

Valid for 50<T<175 K density (kg/m^3)= 5600

C_{NC} =206.6666667+2.284333333*T-.00861*T^2+1.549333333*10^(-5)*T^3-1.048333333*10^(-8)*T^4

Valid for 175<T<500 K density (kg/m^3)=6000

C_{NC} =221.4285714+2.4475*T−.009225*T^2+1.66*10^(−5)T^3−1.123214286*10^(−8)*T^4

Valid for 175<T<500 K density (kg/m^3)=5600

C_{SC}= .008183333*T^3 + .010666667*T*B (J/(kg*K))

Valid for 1<T<15 K density (kg/m^3)=6000

C_{SC} = .008767857*T^3 + .014428571*T*B (J/(kg*K))

Valid for 1<T<15 K density (kg/m^3)=5600

Reference [27]

C_{NC} = 2.3*10^(-3)T^3+.145T

Valid for T<30 K

$$C_{SC}(\theta) = \beta_1\theta^3 + \gamma_1\theta \ [\mathrm{J}\cdot\mathrm{Kg}^{-1}\cdot\mathrm{K}^{-1}]$$

β1 = 2.3*10^(-3)+.435/(Tc0)^2 γ1 = .145*B/Bc

$$B_c(\theta) = (B_{c0}+5)\times\left(1-\frac{\theta}{\theta_{c0}}\right)-5\times\left(1-\frac{\theta}{\theta_{c0}}\right)^{4.5} \qquad B_c(\theta) = B_{c0}\left\{1-\left(\frac{\theta}{\theta_{c0}}\right)^{1.7}\right\}$$

Reference [29]

C_{vSC}=(.87(B/14)*T+4.464*10^(-2)*T^3)*(100^3/1000)/6000 (J/(kg*K))

Valid for density (kg/m^3)=6000

$$C_{vSC}=(.87(B/14)*T+4.464*10\text{^}(-2)*T\text{^}3)*(100\text{^}3/1000)/5600 \text{ (J/(kg*K))}$$

Valid for density (kg/m^3)=5600

$$C_{vNC}=(.87*T+1.38*10\text{^}(-2)*T\text{^}3)*(100\text{^}3/1000)/6000 \text{ (J/(kg*K))}$$

Valid for density (kg/m^3)=6000

$$C_{vNC}=(.87*T+1.38*10\text{^}(-2)*T\text{^}3)*(100\text{^}3/1000)/5600 \text{ (J/(kg*K))}$$

Valid for density (kg/m^3)=5600

2.3.2 Heat conductivity of NbTi

References: Tabulated data from [17][22][40] was fitted to the following equations

$$k = -0.00089085350696236 0T^3 + 0.016706386304553200T^2 - 0.044789876496699500T + 0.068105653491378900$$

Valid 1<T<10K $R^2 = 0.996958$

Reference: tabulated data from [17] Dataset 2 was fitted to the following equations

$$k = 2.707071295071070E\text{-}14T^6 - 1.089542905638570E\text{-}10T^5 + 7.261426646553600E\text{-}08T^4 - 1.768885700474560E\text{-}05T^3 + 1.523577906200000E\text{-}03T^2 + 1.965743220116850E\text{-}02T + 6.411246994511720E\text{-}04$$

Valid for 10<T<100K $R^2 = 0.9994$

Reference: tabulated data from [17] Dataset 2 was fitted to the following equations

$$k = -3.611887887990550E\text{-}08T^3 + 8.451698778158840E\text{-}05T^2 - 1.476621990221600E\text{-}02T + 6.425342077064450$$

Valid 100<T<300 k, $R^2 = 0.9964$

Reference [27]

$$K(\theta) = \frac{L_o \theta}{\rho_{normal}} = 4.375 \times 10^{-2} \theta [\mathrm{W \cdot m^{-1} \cdot K^{-1}}]$$

Valid for 2<T<200 K

2.4 Superconductors and alloys - Nb_3Sn

2.4.1 Specific heat of Nb_3Sn

Nb_3Sn specific heat exhibits the second order phase transition peak, figure ?. The peak occurs at the onset of the superconducting phase [44]. The peak is a strong function of magnetic field. Increasing the magnetic field shifts the superconducting peak to the left. Higher magnetic fields result in a reduction of strand enthalpy.

Nb_3Sn specific heat data shows considerable divergences for both the superconducting state and the normal conducting state, figure ?. For example, at 10 K super conducting data diverges by approximately 19 J/(kg*K) and the normal conducting data diverges by 4 J/(kg·K). Though most data converges by 2 K, figure ?. The primary source of this spread is likely compositional variation of the diffused tin. [47] Different fabrication schemes result in different percentages of tin in Niobium, see figure ?. [46][47][48] Using figure ?, ?, and the Kopp-Neumann law we expect that with a increased Tin content would result in a increased the heat capacity of the normal conducting strand below 100 K and lower the heat capacity above 100 K. It is important to note figure ?, the upper black line represents tin and the lower black line represents niobium. Normal conducting Nb3Sn should lie between these two black lines, however only [16], [39], [27], [25], [17] dataset one lie between these lines.

There is also compositional variation within the filaments. So one would expect the inner and outer layer to have different tin percentage depended properties. Compositional variation in the superconducting state results in a softening of the superconducting peak, figure ?.[48] This is because different alloying percentages have different critical temperatures. [48]

LARP Nb_3Sn cables are fabricated with the internal-tin route. Data from a similarly fabricated cable would be ideal. However, compiled sources seldom present this information with the data. This is because there are a multitude of factors effecting the specific heat measurement. For instance the strands of ITER contain fewer sub-elements then Fermi Lab LARP Nb_3Sn stands.

Fermilab has used references [27] and [39] for their data sets. Reference [17] suggests using the equations form data set two. Without specific compositional knowledge it is suggested that an upper and lower value should be taken from the data.

Reference [16]

$$C_{NC}\ (J/(kg*K)=(11.06T+0.155T^3-0.000065T^5)/99.35$$

Valid for 9<T<18 K, H = 0 T

$$C_{NC}\ (J/(kg*K)= (11\ T + 0.00015568\ T^3)/99.35$$

Valid for T<12K, H = 0 T

Reference [17] Dataset 2

$$C_{p\ NC}= .001*T^3+.1*T\ (J/(kg*K))$$

$$C_{pSC} = (.001+15*.1/Tc^2)T^3+.1(B/Bc20)T\ (J/(kg*K))$$

Valid for 4.2<T< 20 K, 0-7 T

Reference [17] Dataset 2

$$C_{psc}=((A+B)(T/Tc)^3)/8040\ J/(kg*K)$$

$$A=1500C^2/(2D-1)$$

$$C=-.46306-.06783Tc$$

$$D=27.2/(1+.34Tc/Tc0)^2$$

$$B=.0075475Tc^2 \qquad For\ Tc<10K$$

$$B=(.3+.00375Tc^2)/.09937 \quad For\ 10<Tc<20\ K$$

Valid for T<Tcs=7 K

$$C_{p\ Transition\ SC} = (T-Tcs)/(Tc-Tcs)*Cpnorm(T)+(1-(T-Tcs)/(Tc-Tcs))*Cpsc$$

For Tcs=7K<T<Tc=9K [17]

$$C_{pNC} = .0075475*T^2 \qquad T,Tc<10K$$

$$C_{pNC} = (.3+.00375*T^2)/.09937 \qquad 10<T<20K$$

Valid for Tcs<T<Tc

$$C_{pNC} = .0075475T^2 \qquad T,Tc<10K$$

$$C_{pNC} = (.3+.00375T\text{^}2)/.09937 \qquad 10<T<20K$$

Vaild for 20 K >T>Tc

Reference [27]

$$C_{SC} = 4.2*10\text{^}(-3)T\text{^}3+.183T \text{ (J/(kg*K))}$$

Reference [25]

$$C=22.68T\text{^}3 + 988.2 \text{ (J/(m^3*K))}$$

2.4.2 Heat conductivity of Nb_3Sn

Reference [27]

$$\rho_{Nb_3Sn}(\theta) = \min\left(6.0\times\theta^2, 1.75\times\theta^2 - 1.09\times\theta + 3.11\right)[\mathrm{W\cdot m^{-1}\cdot K^{-1}}]$$

Comparison with other data shows that this is inaccurate.

Reference: tabulated data from [22][17] dataset 3&2 was fitted to the following equations

$$k = -1.906620820328610E\text{-}06x^5 + 4.842380418335070E\text{-}05x^4 - 2.014481796734910E\text{-}04x^3 + 6.561801882128290E\text{-}03x^2 - 1.660094463272800E\text{-}02x$$

Valid for 2<T<20 K R^2 = 9.963323874710990E-01

Reference: tabulated data from [17] dataset 3 was fitted to the following equations

$$k = -2.365745696234440E\text{-}13x^6 + 2.418444882194210E\text{-}10x^5 - 9.782152807238660E\text{-}08x^4 + 1.976910315735690E\text{-}05x^3 - 2.039379799956000E\text{-}03x^2 + 8.965442341817190E\text{-}02x + 1.384398172179600E+00$$

Valid for 20<T<300K, R^2 = 9.969291344533260E-01

2.5 Metals - Stainless steel

2.5.1 Specific heat of Stainless Steel 304

References [13]

C (J/(kg*K)=10^(22.0061-127.5528*x+303.6470*x^2-381.0098*x^3+274.0328*x^4-112.9212*x^5+24.7593*Log^6-2.239153*x^7)

Valid for 4<T<300 K

References [18][19]

C=(465*T+.56*T^-2)*10^(-3) (J/(kg*K))

Valid for .1<T<5 K

2.5.2 Heat conductivity of Stainless Steel 304

Reference [13]

$$_{K=10}\ -1.4087+1.3982(\log_{10}T) + 0.2543(\log_{10}T)^2 - 0.6260(\log_{10}T)^3 + 0.2334(\log_{10}T)^4 + 0.4256(\log_{10}T)^5 - 0.4658(\log_{10}T)^6 + 0.1650(\log_{10}T)^7 + -0.0199(\log_{10}T)^8$$

Valid for 1<T<300K, data range 4<T<300K.

2.5.3 Specific heat of Stainless Steel 316LN

Reference [17]

C_p (J/(K*kg))= .48 T + 0.00075 T^3

Valid for 1<T<10K

Tabulated data from [17] was fitted to the following equations

$$C_p = -4.862348815137810E\text{-}06x^5 + 3.444074383409660E\text{-}04x^4 - 7.949135027672580E\text{-}03x^3 + 8.779089919403300E\text{-}02x^2 + 8.688409890100960E\text{-}02x + 6.933646148954720E\text{-}01$$

Valid for 4<T<30 K, R^2 = 9.999999968471320E-01

$$C_p = -2.085598618982040E\text{-}13x^6 - 3.173418409805720E\text{-}09x^5 + 2.874635403118550E\text{-}06x^4 - 9.030428777521940E\text{-}04x^3 + 1.114639598744770E\text{-}01x^2 - 1.982593093780390E+00x + 1.167335212762210E+01$$

Valid for 30<T<300 K, $R^2 = 9.980263310755610E\text{-}01$

2.5.4 Heat conductivity of Stainless Steel 316LN

Reference: tabulated data from [17] dataset 1 & 2 was fitted to the following equations

$$k = -7.594312235277220E\text{-}10x^6 + 9.276437079120190E\text{-}08x^5 - 4.107985169536380E\text{-}06x^4 + 5.916755214064800E\text{-}05x^3 + 1.346998877939300E\text{-}03x^2 + 6.932605599712440E\text{-}02x - 7.753724984925710E\text{-}02$$

Valid for 2<T<50 K $R^2 = 9.999749812317060E\text{-}01$

$$y = 1.025127570486030E\text{-}16x^6 - 5.216067028341940E\text{-}14x^5 - 4.973995535243620E\text{-}10x^4 + 8.397255361034610E\text{-}07x^3 - 5.111722779212390E\text{-}04x^2 + 1.414633090779250E\text{-}01x - 5.224030268254580E\text{-}01$$

Valid for 50<T<300K, $R^2 = 9.990762694676240E\text{-}01$

2.6 Titanium

2.6.1 Specific heat of Ti

Specific Heat of Titanium

Reference [20]

$$C_v=(71000+540*T\text{^}3)/10\text{^}6 \text{ (J/kg*K)}$$

Valid for 0<T<10K=Tmax, From figure ?, it can be see that this equation does not match well with data.

Reference: tabulated data from [19][20][22][24][43] was fitted to the following equations

$$C_p = -4.187501509989030E\text{-}07x^6 + 1.871522770358070E\text{-}05x^5 - 2.772930183532200E\text{-}04x^4 + 2.384488858623970E\text{-}03x^3 - 5.970649812351070E\text{-}03x^2 + 7.977271559915520E\text{-}02x 4.941024663526860E\text{-}03$$

Valid for 1<T<20K, R^2 = 9.999999193097490E-01

$$C_p = 3.639064543627110E\text{-}09x^6 - 6.199156261290500E\text{-}07x^5 + 1.822716742346570E\text{-}05x^4 + 1.351287013378180E\text{-}03x^3 - 2.315364264511310E\text{-}02x^2 + 2.257414222851980E\text{-}01x - 2.365529197364100E\text{-}01$$

Valid for 20<T<70 K, R^2 = 9.999698136624870E-01

$$C_p = 1.345199296029590E\text{-}11x^6 - 1.540964171100770E\text{-}08x^5 + 6.935071989007290E\text{-}06x^4 - 1.516633872522780E\text{-}03x^3 + 1.527963939856350E\text{-}01x^2 - 2.750033746607780E+00x + 9.053558717787490E+00$$

Valid for 70<T<300 K, R^2 = 9.997953432556180E-01

2.6.2 Heat conductivity of Titanium

Reference: tabulated data from [24] was fitted to the following equations

$$k = -4.146563318366350E\text{-}13x^6 + 4.076998258715820E\text{-}10x^5 - 1.570700596710640E\text{-}07x^4 + 3.056163499969890E\text{-}05x^3 - 3.239582681682280E\text{-}03x^2 + 2.007559945258790E\text{-}01x - 1.188200752254610E+00$$

Valid for 20<T<250 K extrapolated to 15K and 300 k [24] Titanium; Rem - Cru, RCl30-B, 4.7% 'Mn, 3.99% Al, .14% C, R^2 = 9.994685516303610E-01

Reference: tabulated data from [43] was fitted to the following equations

$$\boldsymbol{k} = -4.151978065021750E\text{-}06x^3 + 3.976498237367890E\text{-}04x^2 + 4.076654915785600E\text{-}02x - 1.011750881316930E\text{-}01$$

Valid 20<T<100K, Ti (6%Al-4%V), R^2 = 1.000000000000070E+00

$$\boldsymbol{k} = -6.634091860953030E\text{-}07x^3 + 3.785341337428670E\text{-}04x^2 - 4.712159709618850E\text{-}02x + 5.390227558285250E+00$$

Valid for 100<T<300 K, Ti (6%Al-4%V), R^2 = 9.999999999989210E-01

2.7 Niobium

2.7.1 Specific heat of Nb

Can be superconducting, but this data will most likely be unneeded in a magnetic due to the low critical field of niobium.

Reference [20]

$$C_{vNC}=(85000+640*T\text{^}3)/10\text{^}6 \text{ (J/kg*K)}$$

Valid for 0<T<1K

Reference [17]

$$C_{NC}=.0012*T\text{^}3+.085*T \text{ (J/(kg*K))}$$

Valid for 4<T<30 K

References: tabulated data from [24],[20],[19],[17],[15],[14] was fitted to the following equations

$$C_{NC} = 1.854335962359220E\text{-}11x^6 - 1.884320078112840E\text{-}08x^5 + 7.377604897773620E\text{-}06x^4 - 1.366177928330710E\text{-}03x^3 + 1.112919864921200E\text{-}01x^2 - 1.172816904749200E+00x + 3.016294511908200E+00$$

Valid for 30<T<300K, R^2 = 9.988420465017880E-01

$$C_{SC} = -1.765844001244690E\text{-}05x^6 + 5.070570594796210E\text{-}04x^5 - 5.712932158076000E\text{-}03x^4 + 3.481390764500250E\text{-}02x^3 - 7.027787824699770E\text{-}02x^2 + 4.631436617273720E\text{-}02x - 3.082501121753010E\text{-}03$$

Valid for 0<T<9K, R^2 = 9.998435299042530E-01

2.7.2 Heat conductivity of Nb

References: tabulated data from [22][24][17] dataset 3 was fitted to the following equations

$$k = 50$$

Valid for 100<T<300 K

$$k = -5.423769768026070E\text{-}09x^6 + 2.181439693916450E\text{-}06x^5 - 3.560634679318170E\text{-}04x^4 + 3.002985656927430E\text{-}02x^3 - 1.361012454973540E+00x^2 + 3.011317741639440E+01x - 1.639796816323040E+02$$

Valid for 20<T<100 K, R^2 = 9.989740959466120E-01

$$y = -1.632652375249680E\text{-}05x^{6} + 9.958053412759680E\text{-}04x^{5} - 2.289708012806100E\text{-}02x^{4} + 2.437048466409810E\text{-}01x^{3} - 1.272840180504940E+00x^{2} + 8.104067656280450E+00x + 3.269170199763490E+00$$

Valid for 2<T<20 K, R^2 = 9.999997188282660E-01

2.8 Tin

2.8.1 Specific heat of Sn

Reference [20] White Tin

$$C_v=(14700+2210*T\text{^}3)/10\text{^}6 \text{ (J/kg*K)}$$

Valid for 0<T<2K [20]

Reference [24] White Tin: Tabulated data from [24] was fitted to the following equations.

$$C_p \text{ J/(kg*K)} = 8.651957877248150E\text{-}05x^{6} - 3.349530150529740E\text{-}03x^{5} + 4.686885801594090E\text{-}02x^{4} - 2.867543747755120E\text{-}01x^{3} + 8.542735671570510E\text{-}01x^{2} - 1.137213002845870E+00x + 5.440992180789550E\text{-}01$$

Valid for 1<T<10K, R^2=9.999989331180580E-01

$$C_p \text{ J/(kg*K)} = y = 1.133333333331880E\text{-}04x^{4} - 1.099999999998150E\text{-}02x^{3} + 3.971666666655410E\text{-}01x^{2} - 2.724999999988600E+00x + 5.500000000055960$$

Valid for 10<T<30K, R^2=9.999999999912710E-01

$$C_p = 10^{a+b\cdot x-c\cdot x^2+d\cdot x^3+e\cdot x^4+f\cdot x^5+g\cdot x^6+h\cdot x^7+i\cdot x^8+j\cdot x^9+k\cdot x^{10}+l\cdot x^{11}} \frac{J}{kg\cdot K}$$

where x= $\log_{10}(T)$. The coefficients for equation are given in table 1.

TABLE 1

a	1.55718652083960E-05
b	3.28428483506997E-05
c	7.06924168936027E-05

d	1.54816059121578E-04
e	6.07112089853614E-01
f	-4.24278700670351E-01
g	4.95713065603732E-02
h	5.85746556006985E-02
i	6.28869701778489E-02
j	5.16442717073555E-03
k	-1.46819770508911E-03
l	-1.19012436777440E-06

Valid for 25<T<300 K R^2=0.999695774143388

2.8.2 Heat conductivity of Tin

Tin heat conductivity increases at low temperatures, figure ?.

Reference [24] White Tin: Tabulated data from [24] was fitted to the following equations.

$$k = -4.879359708933550E\text{-}02x + 1.903247692450810E+02$$

Valid for 35<T<200K, Tin: 99.995% pure, single crystal, All data between 35<T<295 K is extrapolated, $R^2 = 5.484245412533090E\text{-}01$

$$k = 180\ W/(m*K)$$

Valid for 200<T<300K, extrapolated data.

$$k = 1.139646700283330E\text{-}04x^6 - 1.543856378711080E\text{-}02x^5 + 8.544894414597910E\text{-}01x^4 - 2.485223028318840E+01x^3 + 4.043972973968770E+02x^2 - 3.550721992769150E+03x + 1.371471776541710E+04$$

Valid for 10<T<30K, pure, single crystal, $R^2 = 1.000000000177030$

$$k = -1.420168159820610E\text{-}01x^6 + 5.822864544461480E+00x^5 - 9.007839438028170E+01x^4 + 6.683951905751600E+02x^3 - 2.521412335171820E+03x^2 + 4.570981105430050E+03x - 5.394627478686740E+02$$

Valid for 2<T<10 K, pure, single crystal, $R^2 = 9.999999492963420E\text{-}01$

2.9 Copper

Only sparse data was gathered on copper. Significant data can still be extracted from references.

2.9.1 Specific heat of Copper

Datasets of specific heat of copper converge. Reference 13 can be used with confidence.

Reference [13]

C_p=10^(-1.91844-0.15973*x + 8.61013*x^2 -18.996*x^3+ 21.9661*x^4-12.7328*x^5 +3.54322*x^6-0.3797*x^7)

Where x = Log_{10}(T) Valid for 4<T<300 K

2.9.2 Heat conductivity of Copper

Great caution need to be taken when using data on the thermal conductivity of copper. Copper conductivity is a strong function of RRR effects and magnetic fields. Reference [13] website and [17] contain detailed data.

2.10 Bronze

Bronze is an alloy of copper and tin. Copper content usually varies by 30 to 55 %. [33].

2.10.1 Specific heat of bronze

Specific Heat of Bronze

Specific heat of bronze is expected to lie between copper and tin.

Reference [17] Dataset2

C_v=(1/M)(γ*T+D(x))
M(Sn)=1.187*Sn+.6354*(100-Sn)
γ= .698+.00911*Sn-.00128*Sn^2+6.54*10^(-5)*Sn^3

θ(Sn)= 344-3.11*Sn

x=θ(Sn)/T

Where Sn is % tin content.

TABLE 2 (table description)

Where debye function D(x) is given numerically	
x	D(x) (J/kmol/K)
0	24915.72
1	23723.28
2	20585.28
3	16526.8
4	12535.26
5	9192.248
6	6619.088
7	4757.208
8	3443.432
9	2527.136
10	1891.168
11	1443.48
12	1117.128
13	882.824
14	707.096
15	573.208
16	472.792
17	395.388
18	333.046
19	283.257
20	243.09
22	182.422
26	110.458
30	71.965

Valid for 0<T<300 K, by comparison to other data figure ?, this equation works well between 0%<Sn<60%.

2.10.2 Heat conductivity

$y = 10$ (.4145+*1.563*($\log_{10}T$) -.2285($\log_{10}T$)^2 -.3234*Sn+.02500Sn^2) (W/(K*m))

Where Sn is in wt%, valid for 1<T<300 k, No significant effect of annealing, Sn<7.3wt%[17]

3 Bibliography

‘[1] Baudouy B., „Kapitza resistance and thermal conductivity of Kapton in superfluid helium”, Cryogenics 43(2003), 667-672,

'[2] Nacher PJ et al.,” Heat exchange in liquid helium through thin plastic foils”, Cryogenics 32 (1992),

'[3] Baudouy B., Polinski J., „Thermal conductivity and Kapitza resistance of epoxy resin fiberglass tape at superfluid helium temperature”, Cryogenics 49(2009), 138-143

'[4] Arp V.D., “Stability and thermal quenches in force-cooled superconducting cables,” Proc. of 1980 Superconducting MHD Magnet Design Conference, MIT, 142(1980)

'[4-bis] P.P. Granieri et al, „ Stability analysis of the LHC cables for transient heat depositions”, IEEE Trans. Appl. Supercond., vol. 18, No. 2 (2008).

'[5] A. Kashani and S.W.Van Sciver, „High heat flux Kapitza conductance of technical copper with several different surface preparations”, Cryogenics 25 (1985),Issue 5, 238-242

'[6] D. Camacho et al.,”Thermal characterization of the HeII LHC heat exchanger tube”, LHC Project Report 232, 1998.

'[7] Ch. Darve et al., "Experimental Investigations of He II Heat
Transfer through a Short Section of LHC inner Triplet
Quadrupole Heat Exchanger", Fermilab-TD-00-066 (2000)

'[8] Lawrence et al., „ The thermal conductivity of Kapton HN between 0.5 and 5 K”, Cryogenics 40 (2000), 203-207,

'[9] Barucci et al, „Low temperature thermal conductivity of Kapton and Upilex”, Cryogenics 40 (2000), 145-147,

'[10] Handbook on Materials for S.C. Machinery, NBS Boulder (yellow book), 1977 - (from Cryocomp ver.3.0)

'[11] Cryocomp ver. 3.0

'[12] Knapp G.S. et al, "Phonon Properties of A-15 Superconductors obtained from Heat Capacity Measurements", Phys. Rev. B, No.9, (1976), 3783-3789

'[13] NIST - E.D. Marquardt et al., " Cryogenic material properties database", in Proc. 11th Int. Cryocooler Conf., Keystone, 2000
http://cryogenics.nist.gov/MPropsMAY/material%20properties.htm

'[14] Leopold H. A., Boorse, H. A., "Superconducting and Normal Specific Heats of a Single Crystal of Niobium" phys. rev., 134, 1322, 1964 http://prola.aps.org/pdf/PR/v134/i5A/pA1322_1

'[15] Igor S. Grigoriev,Evgeni Z. Meilikhov, "Handbook of physical quantities" pg 261

'[16] M. N. Khlopkin "The specific heat of Nb3Sn in magnetic fields up to 19 T" Sov.Phys.JETP.63.1.164.1986 (Multiple additional data in references that shows discrepancy)

'[17] P. Bauer,H. Rajainmaki, E. Salpietro "4. EFDA Material Data Compilation for Superconductor Simulation" EFDA CSU, Garching, 04/18/07

'[18] C. Hagmann. P.L. Richards, "Specific heat of stainless steel below T = 1 K" Cryogenics 35, 345 (1995) http://www.sciencedirect.com/science/article/pii/001122759595355I

'[19] Guglielmo Ventura, Lara Risegari "The art of cryogenics: low-temperature experimental techniques" pg65, pg72 http://books.google.com/books?id=4kvzBRUuGDkC&pg=PA64&dq=schottky+specific+heat&hl=en&ei=CGMTTtGKFoeQsQLAwdDUDw&sa=X&oi=book_result&ct=result&resnum=2&ved=0CCsQ6AEwATgK#v=onepage&q=schottky%20specific%20heat&f=false

'[20] Robert J. Corruccini, John J. Gniewek, "Specific Heat and enthalpies of technical solids at low temperatures A compilation from the Literature" U.S. Department of Commerce National Bureau of Standards 1960. http://digicoll.manoa.hawaii.edu/techreports/PDF/NBS21.pdf

'[21] B. J. P. Baudouy, F. p. Juster, C. Meuris, l. Vieillard, M. X. Francois, "steady-state heat transfer in He II through porous superconducting cable insulation" CEA, Dapnia/STCM, CE-Saclay, Gif sur Yvette, 91191, France

'[22] Lucio Rossi, Massimo Sorbi: CARE-Note-2005-018-HHH "MATPRO: A Computer Library of Material Property at Cryogenic Temperature.", January 16, 2006. Superconductors Database beta http://sdb-server.cern.ch/mediawiki/index.php/Category:Materials

'[23] L. J. Vieland, A. w. Wicklund, "Specific heat of Niobium-Tin*", Physical Review Volume 166, Number 2, February 10 1968

'[24] Jensen, J. E., Tuttle, W. A., Stewart, R. B., Brechna, H., Prodell, A.G.: "Selected Cryogenic Data Book", Brookhaven National Laboratory, 1980 http://materialdatabase.magnet.fsu.edu/CryoDatahandBook/

'[25] Dr.-Ing. Stephan Russenschuck "Field Computation for Accelerator Magnets: Analytical and Numerical Methods for Electromagnetic Design and Optimization" "Appendix A

Material Property Data for Quench Simulations" Print ISBN: 9783527407699 Online ISBN: 9783527635467 DOI: 10.1002/9783527635467

http://onlinelibrary.wiley.com/book/10.1002/9783527635467
http://onlinelibrary.wiley.com/doi/10.1002/9783527635467.app1/pdf

'[26] Robert J Corruccini, John J Gniewek, "Thermal Expansion of Technical Solids at Low Temperatures: A Compilation From the Literature" 1961-05-19 U.S. Department of Commerce. National Bureau of Standards http://digicoll.manoa.hawaii.edu/techreports/Pages/viewtext.php?s=browse&tid=215&route=browseby.php&city=NBS+Monograph+29&by=city&s=browse

'[27] Kim, S-W.: Material Properties for Quench Simulation (Cu, NbTi and Nb3Sn), FNAL TD-00-041, Batavia, 2000

'[28] D. J. Benford, T. Powers, S. H. Mosely, "Thermal conductivity of Kapton tape"

'[29] J.B. Jeanneret————————————————,x, D. Leroyy, L. Oberliy, T. Trenklerz "QUENCH LEVELS AND TRANSIENT BEAM LOSSES IN LHC MAGNETS" LHC Project Report 44, Geneva, 29 July 1996

'[30] Linda Imbasciati "Studies of quench Protection in Nb3Sn Superconducting Magnets for Future Particle Accelerators" Fermi Natinonal accelerator laboratory technical division, development and test dept. under the dupervision of Dr. Pierre Bauer Milan, Italy

'[31] Hyper physics Niobium-Tin Superconductor http://hyperphysics.phy-astr.gsu.edu/hbase/solids/scex2.html

'[32] Private correspondence with Composite Technology Development, inc. Engineered Material solutions http://www.ctd-materials.com/papers/menu.php

'[33] A. den Ouden and J. M. von Oort et al., “Thermal conduction in fully impregnated Nb Sn windings for LHC type of dipole magnets,” Adv. Cryo. Eng. (Materials), vol. 38, pp. 635–642, 1992.

'[34] DuPon Kapton HN polyimide film Technical Data Sheet http://www2.dupont.com/Kapton/en_US/assets/downloads/pdf/HN_datasheet.pdf

'[35] DuPont High Performance Films Technical Information Kapton JP http://www.welchfluorocarbon.com/DuPontHighPerformanceFilm_TeflonFEPTeflonPFATefzelETFETedlarPVFKaptonPI/H-62026-2_DuPontKaptonJPTechnicalInformation.pdf

'[36] EFDA JET Figures Database http://figures.jet.efda.org/thumbnails/W-2002/301-400/JG02.387/JG02.387-3c.1500.1500.jpg thermal conductivity

'[37] P. Bauer, P. Bruzzone, A. Portone, F. Roth, M. Vogel, A. Vostner, K. Weiss Review of material properties, past experiences, procedures, issues and results for a possible solder filled cable as Plan B conductor for the EFDA dipole magnet (Draft Vs 1) European Fusion

Development Agreement Close Support Unit - Garching March 28th 2007 http://infoscience.epfl.ch/record/121363/files/lrp_830_07.pdf

'[38] Fischer E1, Kurnyshov R2 and Shcherbakov P3,4 Analysis of Coupled Electromagnetic-Thermal Effects in Superconducting Accelerator Magnets doi:10.1088/1742-6596/97/1/012261 Journal of Physics: Conference Series 97 (2008) 012261 http://iopscience.iop.org/1742-6596/97/1/012261/pdf/1742-6596_97_1_012261.pdf

'[39] Eric Marscin,Ryuji Yamada "3D ANSYS Quench Simulation Program with Full Magnet Coil Geometry" Fermi National Accelerator Laboratory TD-03-043 09/08/03

'[40] Pierre Bauer, "Stability of Superconducting Strands for Accelerator Magnets," Ph.D. thesis, Technische Universitat Wien, 1998. pg 63

'[41] MatWeb Material property data http://www.matweb.com/search/DataSheet.aspx?MatGUID=63dbf7fcefbd42b99a190cad7e109056 http://www.matweb.com/search/DataSheet.aspx?MatGUID=ab35b368ab9c40848f545c35bdf1a672

'[42] NBS Monograph 132 page 643

'[43] Jack W. Ekin "Expermental Techniques for Low Temperature Measurements" ISBN 0-19-857054-6 978-0-19-857054-7 Oxford University Press 2006

'[44] Richard P. Reed, Alan F. Clark "Materials at low temperatures" Natinal Bureau of Standard 1983 ISBN 0-87170-146-4

'[45] Michael McClintock "Cryogenics" Reinhold Pub. Corp., 1964 - Technology & Engineering "Note that not all data has been extracted."

'[46] A Godeke "A review of the properties of Nb3Sn and their variation with A15 composition morphology and strain state" Ernest Orlando Lawerence Berkeley National Laboratory, Berkeley, CA 94720, USA 26 June 2006

'[47] Private correspondence with Lance Cooley at Fermi National Accelerator Laboratory August 8, 2011 ldcooley@fnal.gov

'[48] C D Hawes1, P J Lee and D C Larbalestier "Measurements of the microstructural, microchemical and transition temperature gradients of A15 layers in a high-performance Nb3Sn powder-in-tube superconducting strand" The Applied Superconductivity Center, The University of Wisconsin-Madison,Madison, WI 53706-1609, USA doi: 10.1088/0953-2048/19/3/004 http://iopscience.iop.org/0953-2048/19/3/004/

'[49] Private correspondence With Dariusz Bocian at Fermi at Fermi National Accelerator Laboratory

'[50] Adam L. Woodcraft, Adam Gray "A low temperature thermal conductivity database" doi:10.1063/1.3292433 December 16, 2009 http://scitation.aip.org/getabs/servlet/GetabsServlet?prog=normal&id=APCPCS001185000001000681000001&idtype=cvips&gifs=yes

'[51] D. L. Rule, D. R. Smith and L. L. Sparks "THERMAL CONDUCTIVITY OF A POLYMIDE FILM BETWEEN 4.2 AND 300K, WITH AND WITHOUT ALUMINA PARTICLES AS FILLER" August 1990

4 Appendix

4.1 Appendix 1

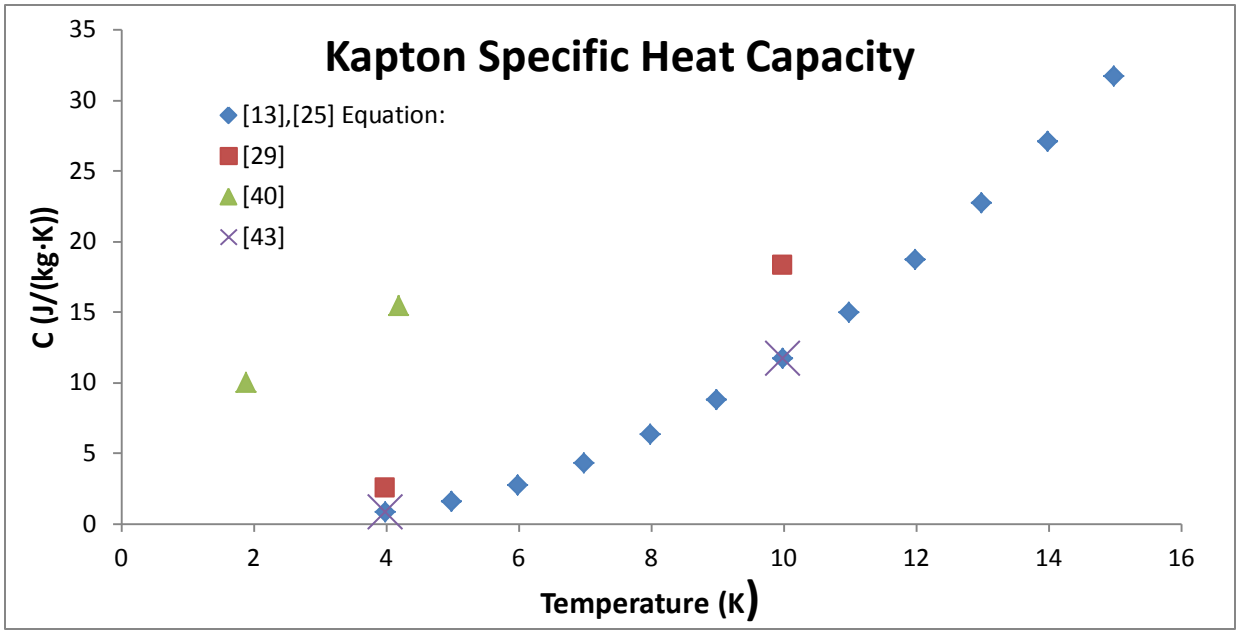

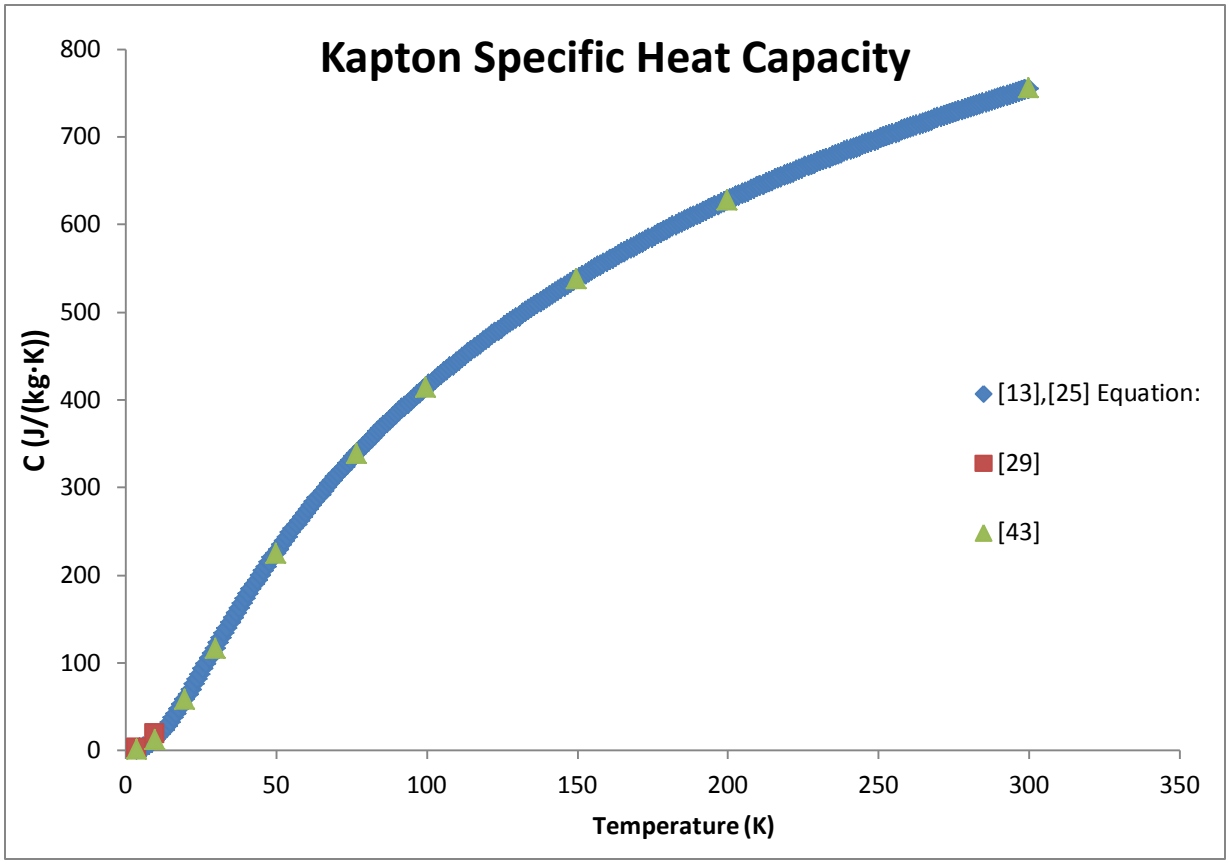

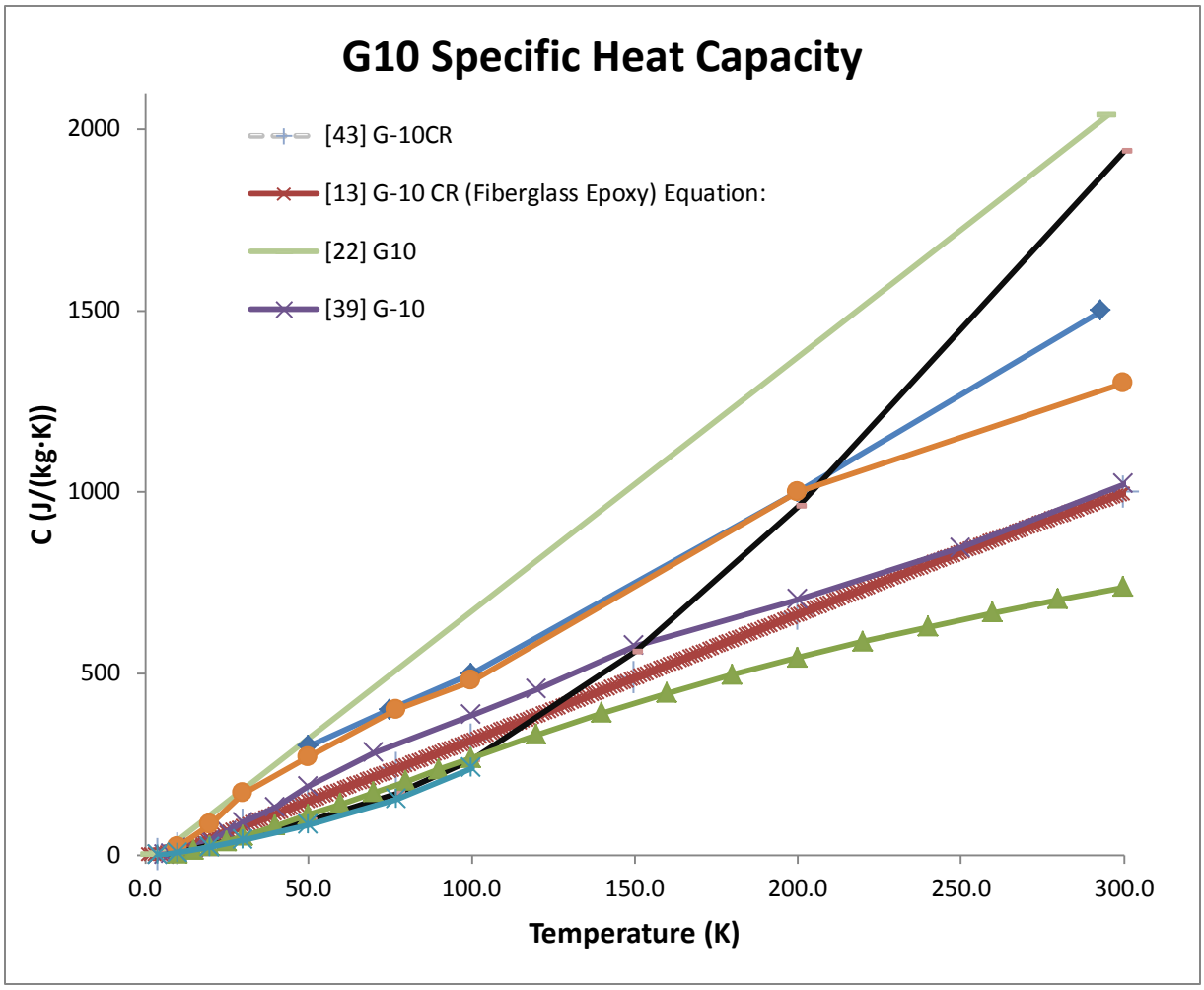
G10 Specific Heat Capacity
[43] G-10CR
[13] G-10 CR (Fiberglass Epoxy) Equation:
[22] G10
[39] G-10
C (J/(kg·K))
Temperature (K)
0
500
1000
1500
2000
0.0
50.0
100.0
150.0
200.0
250.0
300.0

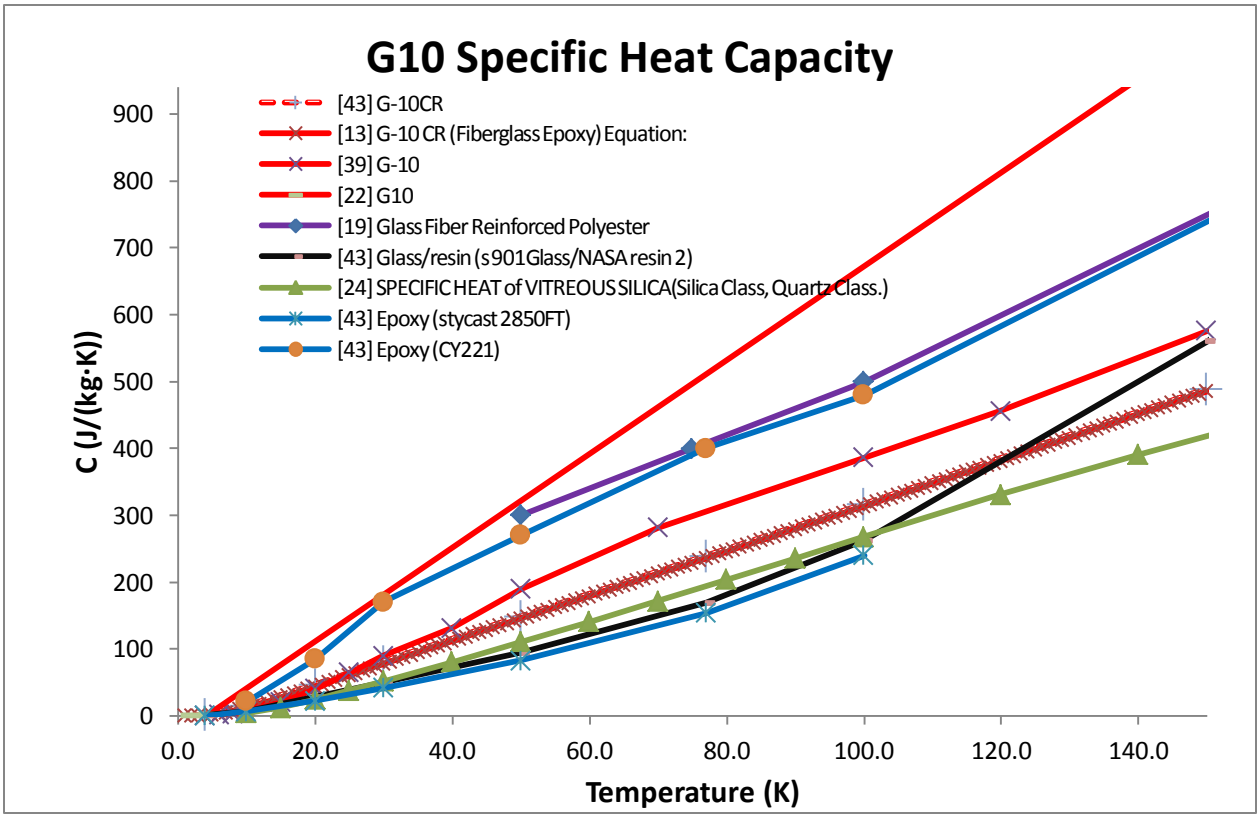
G10 Specific Heat Capacity
[43] G-10CR
[13] G-10 CR (Fiberglass Epoxy) Equation:
[39] G-10
[22] G10
[19] Glass Fiber Reinforced Polyester
[43] Glass/resin (s901Glass/NASA resin 2)
[24] SPECIFIC HEAT of VITREOUS SILICA(Silica Class, Quartz Class.)
[43] Epoxy (stycast 2850FT)
[43] Epoxy (CY221)
C (J/(kg·K))
Temperature (K)
0
100
200
300
400
500
600
700
800
900
0.0
20.0
40.0
60.0
80.0
100.0
120.0
140.0

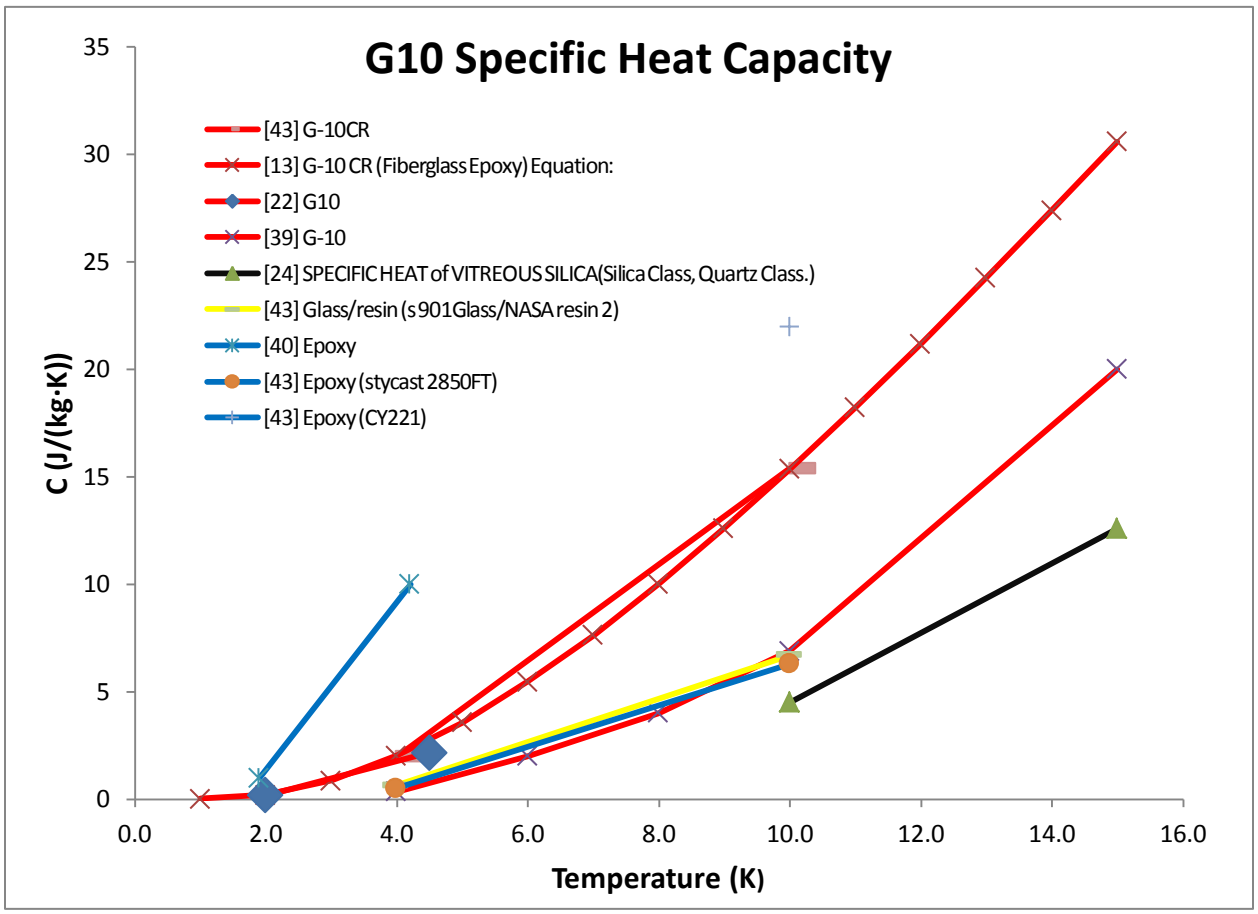
G10 Specific Heat Capacity
[43] G-10CR
[13] G-10 CR (Fiberglass Epoxy) Equation:
[22] G10
[39] G-10
[24] SPECIFIC HEAT of VITREOUS SILICA(Silica Class, Quartz Class.)
[43] Glass/resin (s901Glass/NASA resin 2)
[40] Epoxy
[43] Epoxy (stycast 2850FT)
[43] Epoxy (CY221)
C (J/(kg·K))
Temperature (K)
0
5
10
15
20
25
30
35
0.0
2.0
4.0
6.0
8.0
10.0
12.0
14.0
16.0

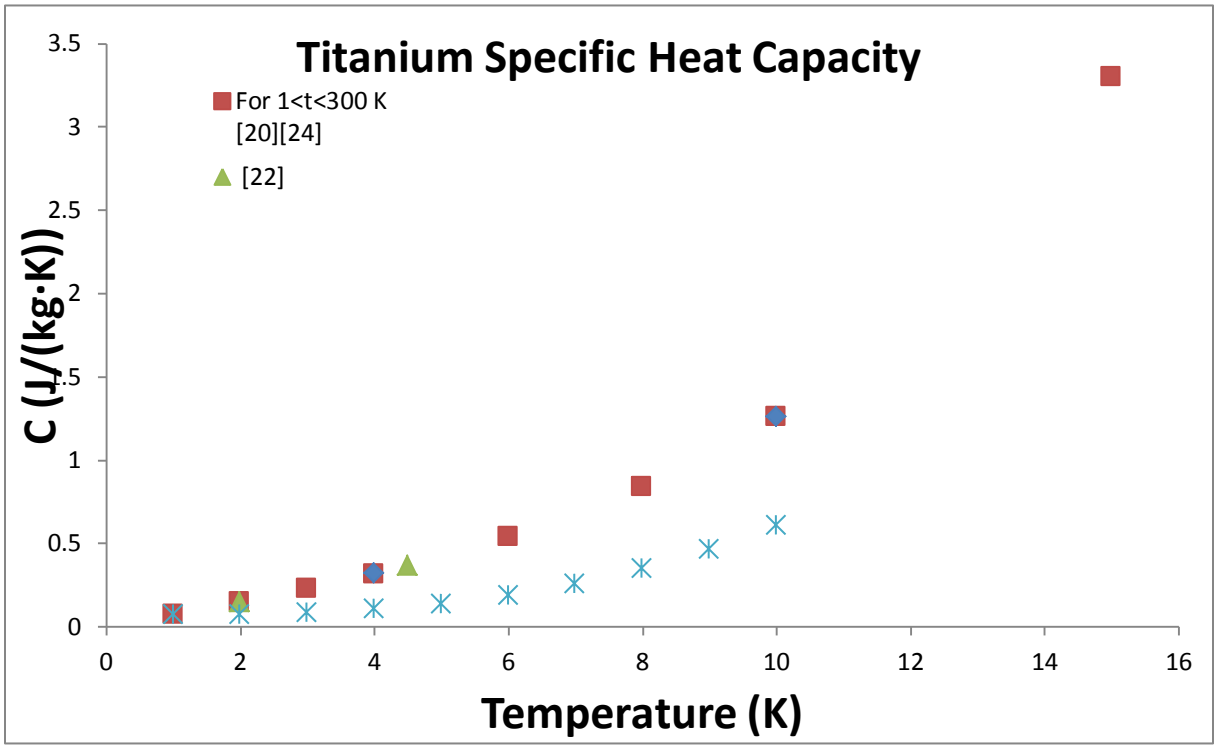
Titanium Specific Heat Capacity
For 1<t<300 K
[20][24]
[22]
C (J/(kg·K))
Temperature (K)
0
0.5
1
2
2.5
3
3.5
0
2
4
6
8
10
12
14
16

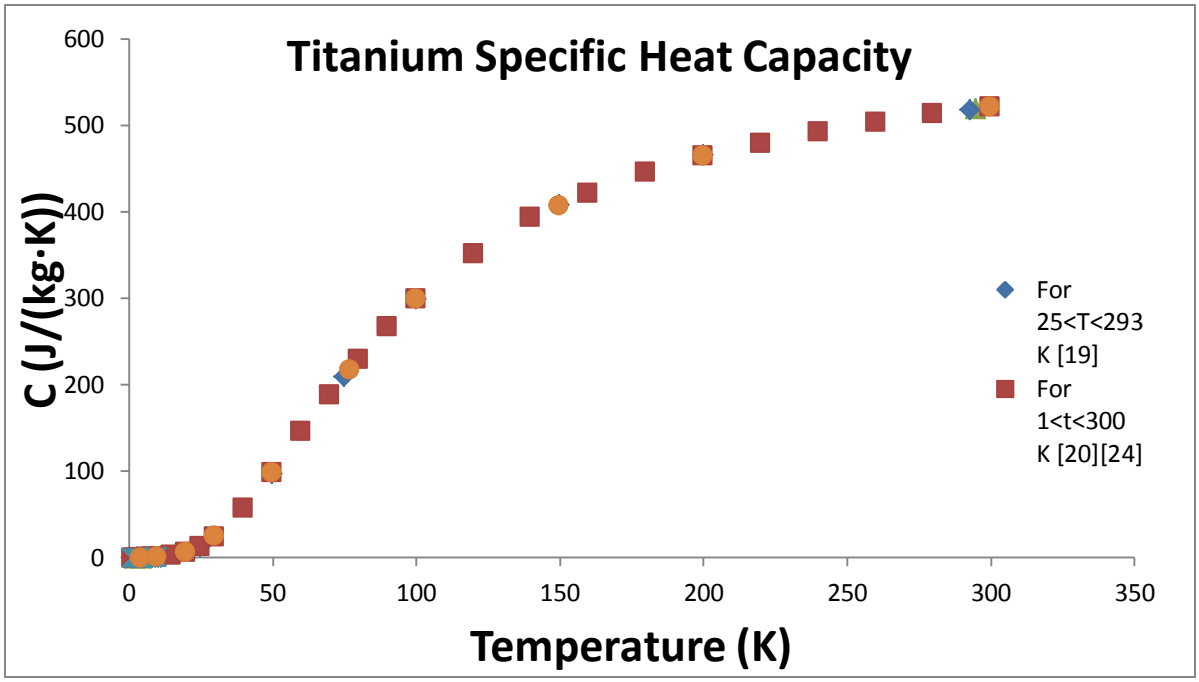
Titanium Specific Heat Capacity
C (J/(kg·K))
Temperature (K)
600
500
400
300
200
100
0
0
50
100
150
200
250
300
350
For 25<T<293 K [19]
For 1<t<300 K [20][24]

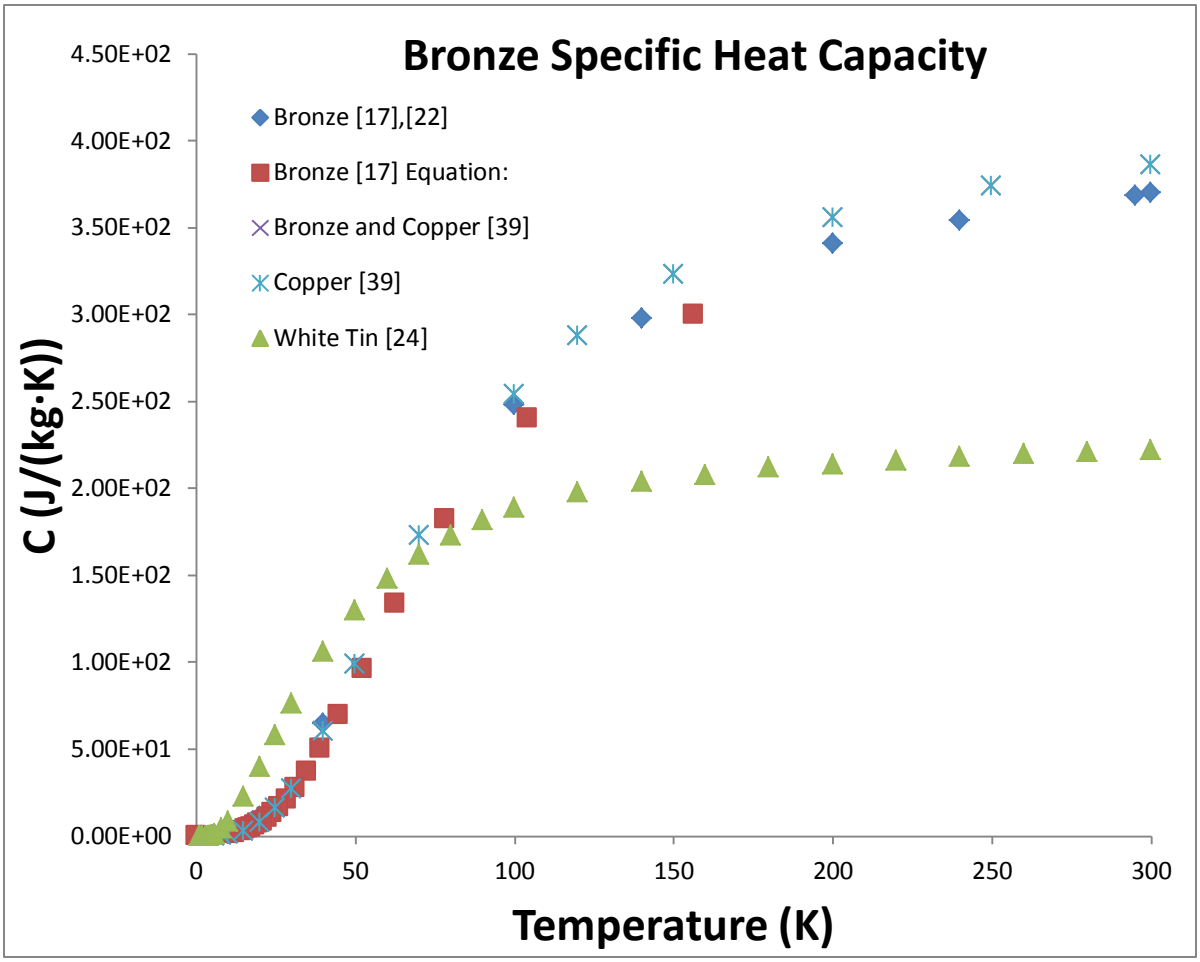
Bronze Specific Heat Capacity
C (J/(kg·K))
Temperature (K)
4.50E+02
4.00E+02
3.50E+02
3.00E+02
2.50E+02
2.00E+02
1.50E+02
1.00E+02
5.00E+01
0.00E+00
0
50
100
150
200
250
300
Bronze [17],[22]
Bronze [17] Equation:
Bronze and Copper [39]
Copper [39]
White Tin [24]

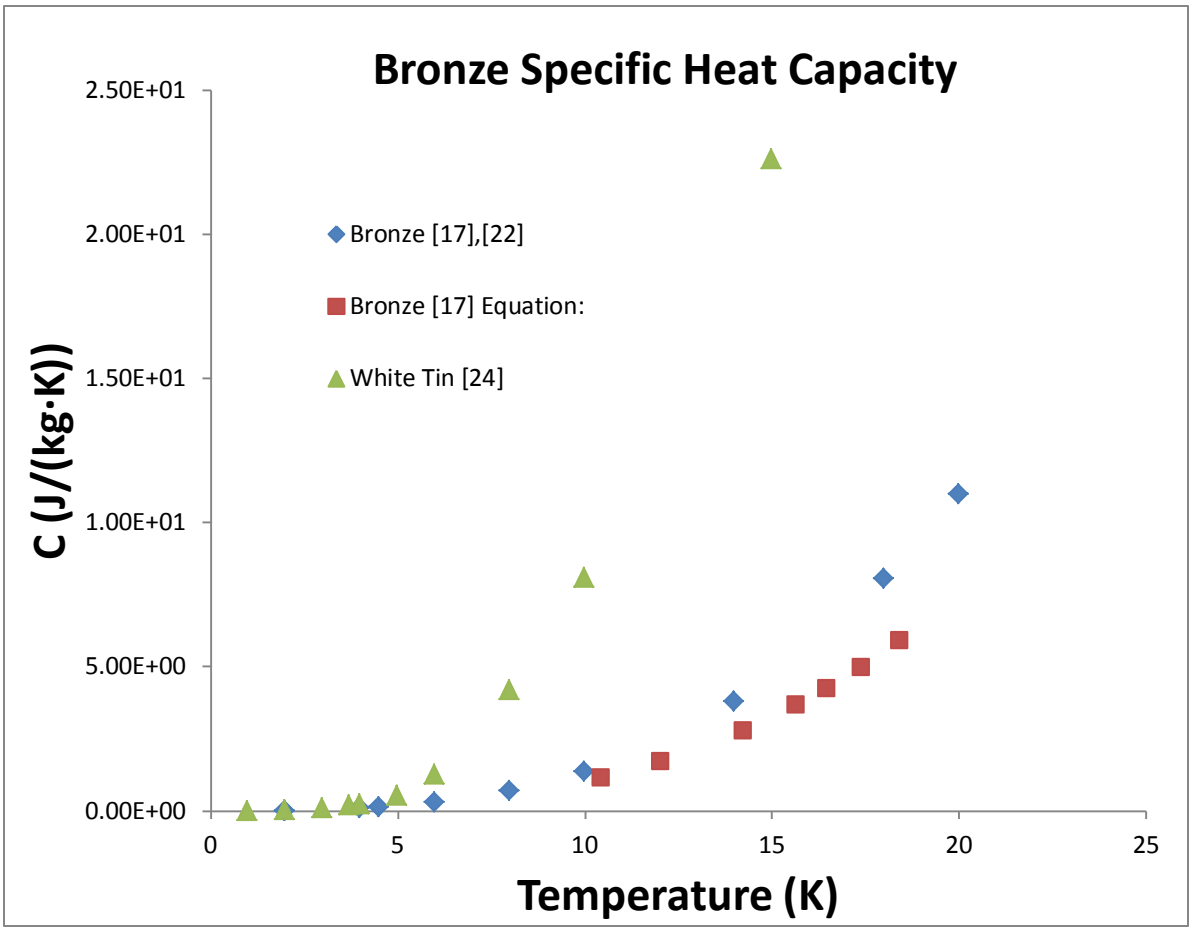
Bronze Specific Heat Capacity
2.50E+01
2.00E+01
1.50E+01
1.00E+01
5.00E+00
0.00E+00
C (J/(kg·K))
0
5
10
15
20
25
Temperature (K)
Bronze [17],[22]
Bronze [17] Equation:
White Tin [24]

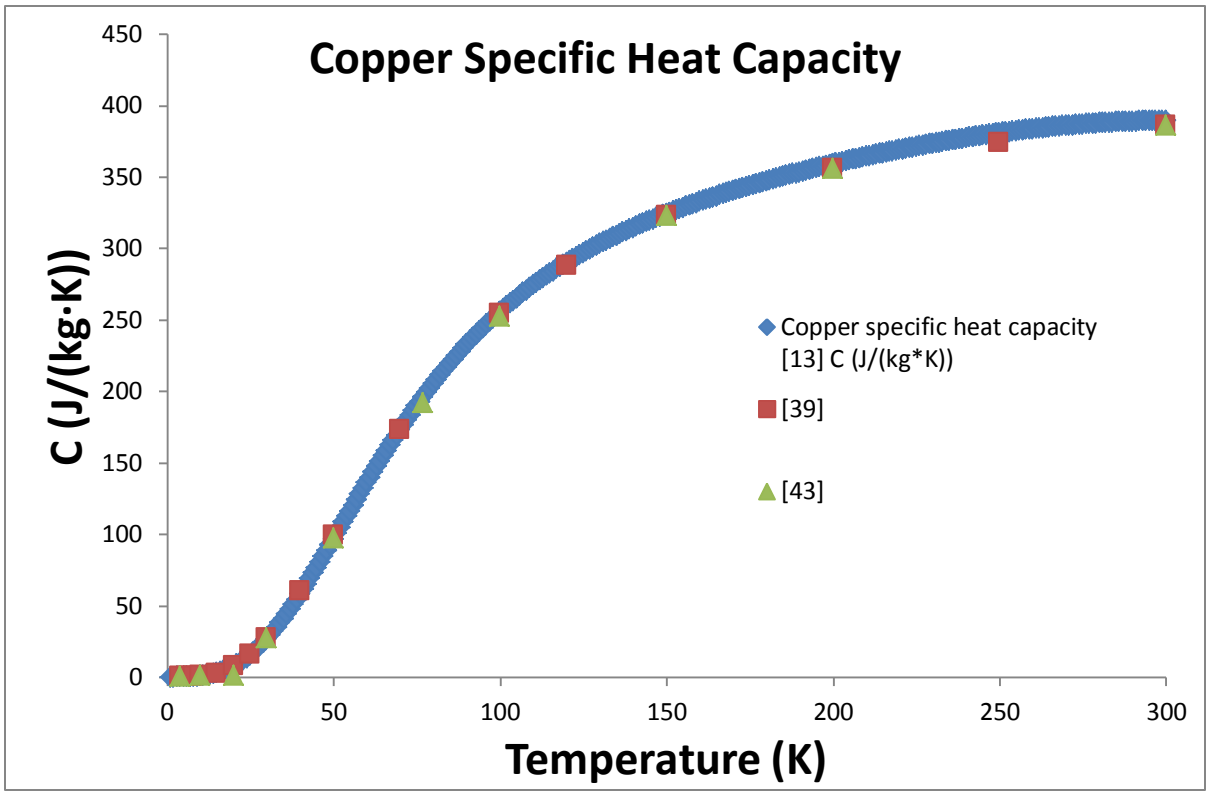
Copper Specific Heat Capacity
450
400
350
300
250
200
150
100
50
0
C (J/(kg·K))
0
50
100
150
200
250
300
Temperature (K)
Copper specific heat capacity [13] C (J/(kg*K))
[39]
[43]

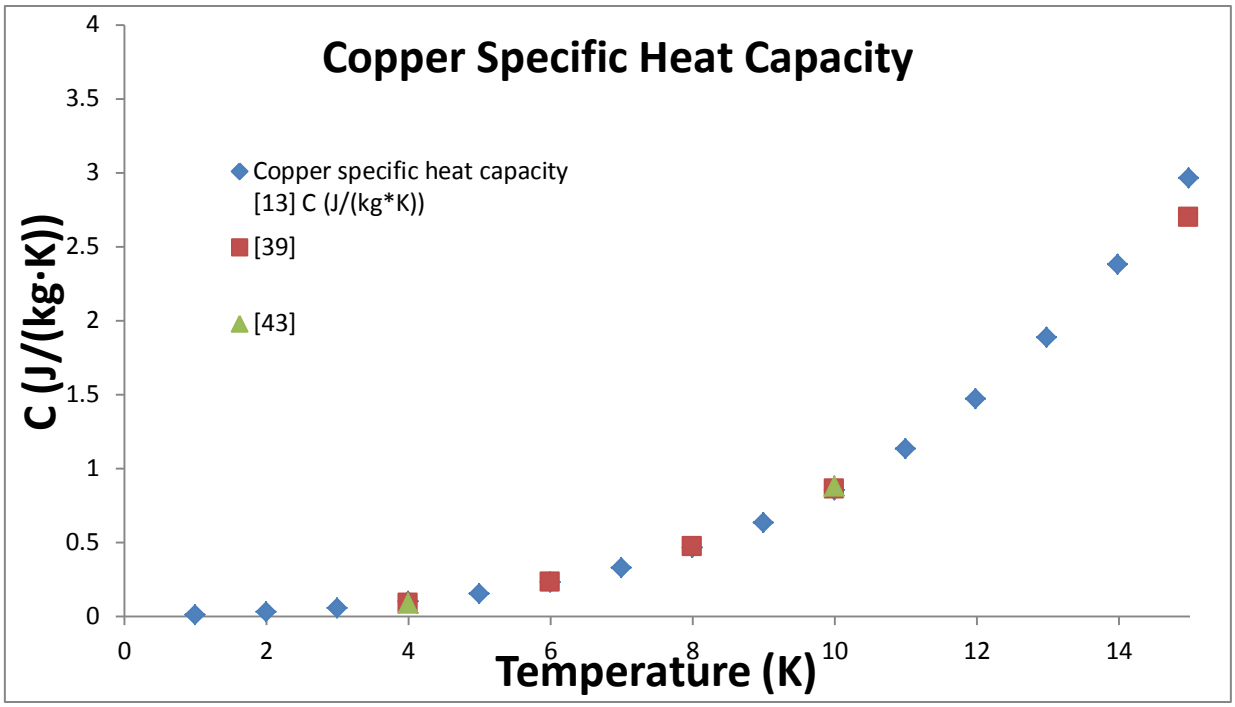
Copper Specific Heat Capacity
Copper specific heat capacity [13] C (J/(kg*K))
[39]
[43]
C (J/(kg·K))
Temperature (K)
0
0.5
1
1.5
2
2.5
3
3.5
4
0
2
4
6
8
10
12
14

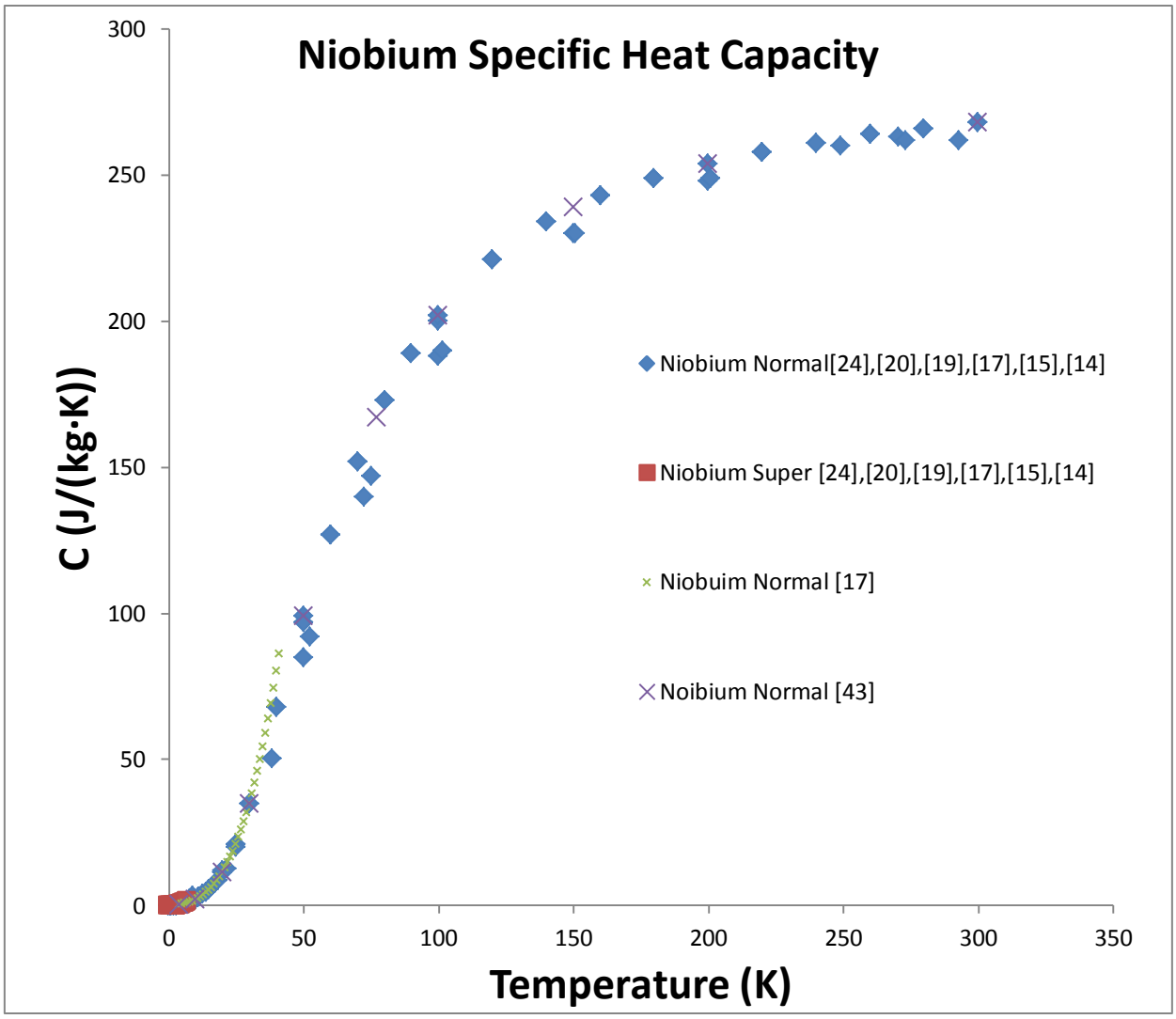
Niobium Specific Heat Capacity
Niobium Normal[24],[20],[19],[17],[15],[14]
Niobium Super [24],[20],[19],[17],[15],[14]
Niobuim Normal [17]
Noibium Normal [43]
C (J/(kg·K))
Temperature (K)
0
50
100
150
200
250
300
350

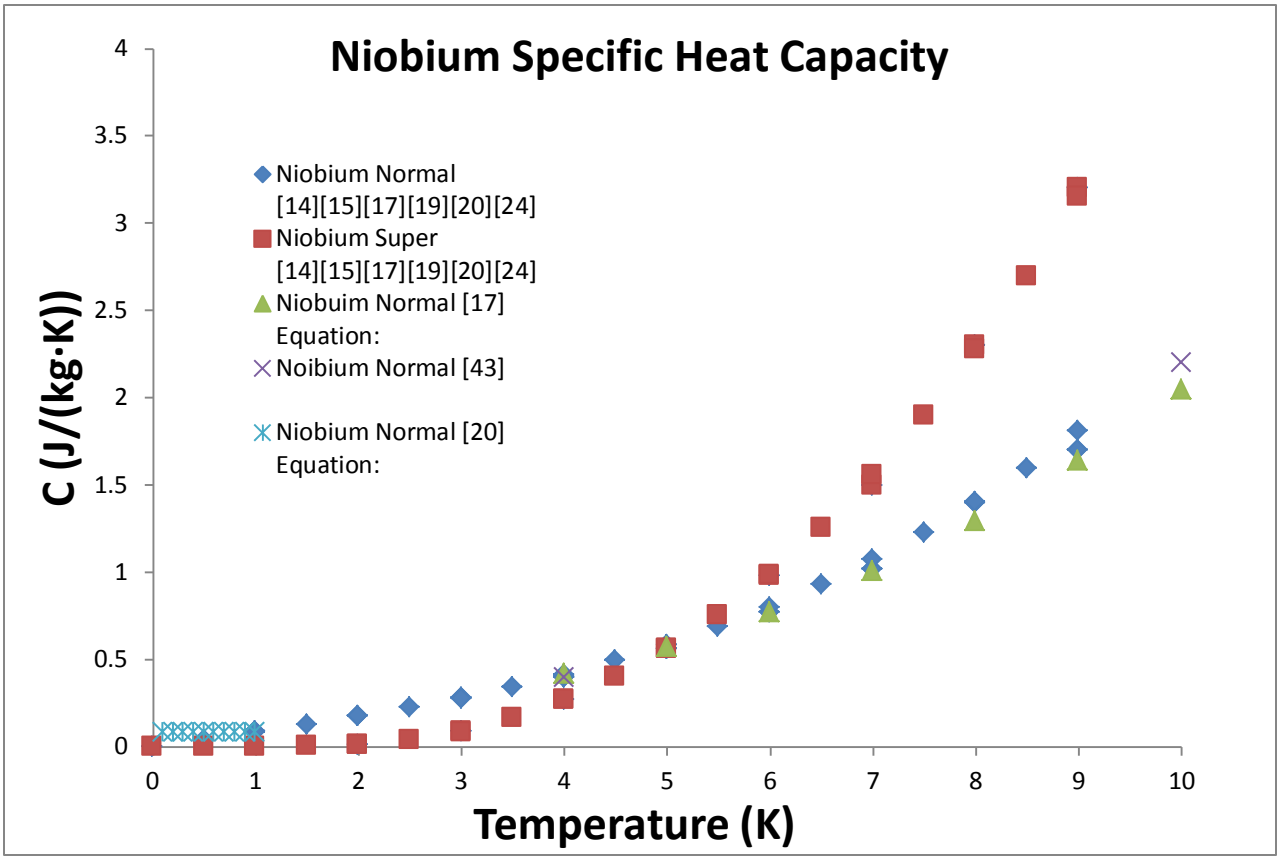
Niobium Specific Heat Capacity
C (J/(kg·K))
Temperature (K)
Niobium Normal [14][15][17][19][20][24]
Niobium Super [14][15][17][19][20][24]
Niobuim Normal [17] Equation:
Noibium Normal [43]
Niobium Normal [20] Equation:
0
0.5
1
1.5
2
2.5
3
3.5
4
0
1
2
3
4
5
6
7
8
9
10

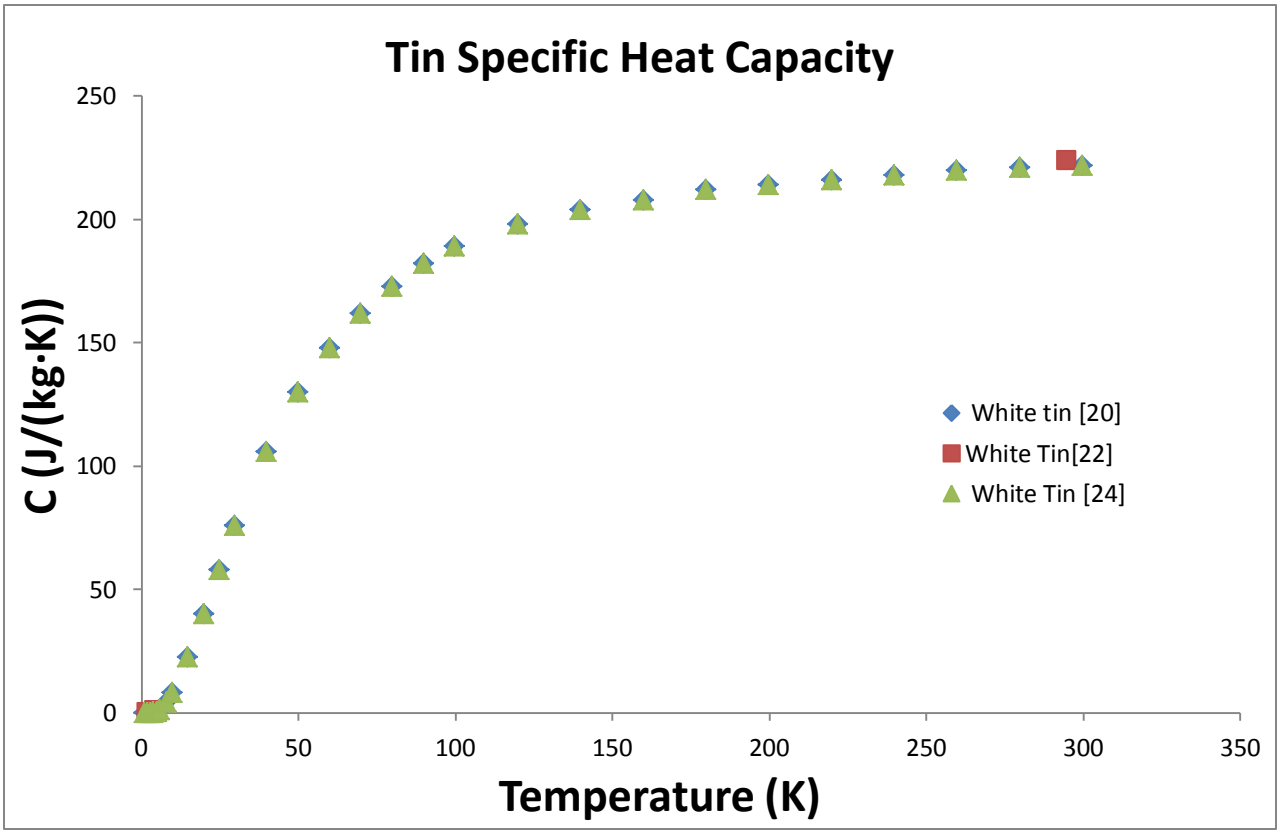
Tin Specific Heat Capacity
C (J/(kg·K))
Temperature (K)
White tin [20]
White Tin[22]
White Tin [24]
0
50
100
150
200
250
300
350

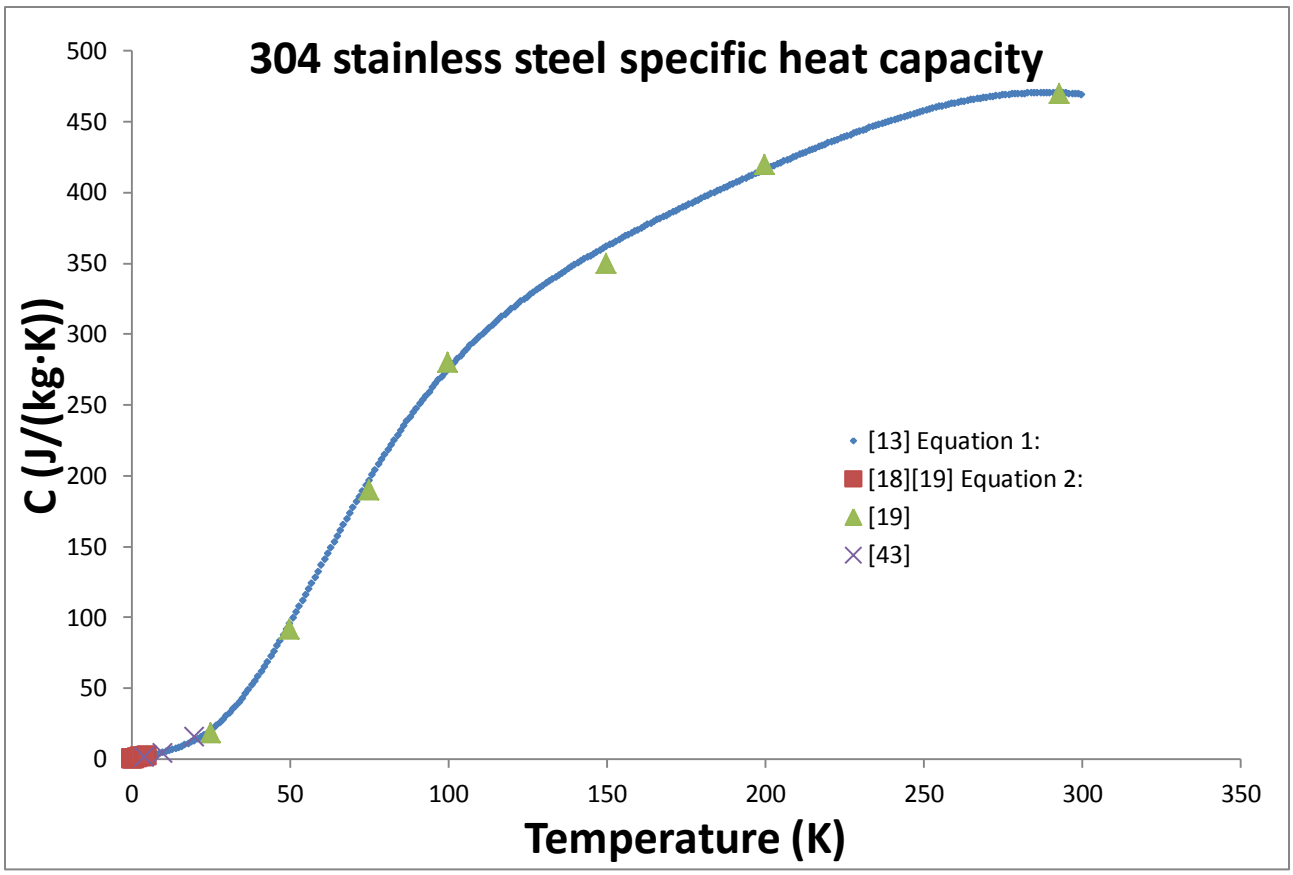
304 stainless steel specific heat capacity
C (J/(kg·K))
Temperature (K)
[13] Equation 1:
[18][19] Equation 2:
[19]
[43]
0
50
100
150
200
250
300
350
400
450
500

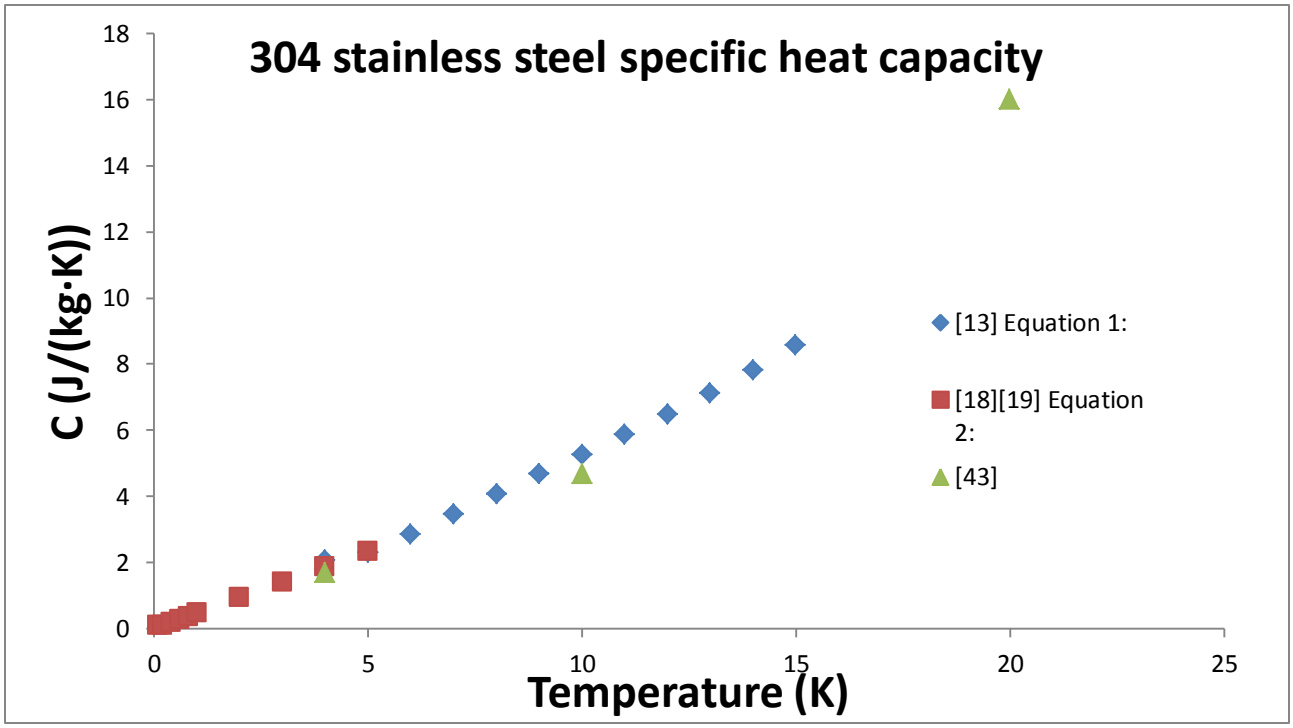
304 stainless steel specific heat capacity
C (J/(kg·K))
Temperature (K)
[13] Equation 1:
[18][19] Equation 2:
[43]
0
2
4
6
8
10
12
14
16
18
0
5
10
15
20
25

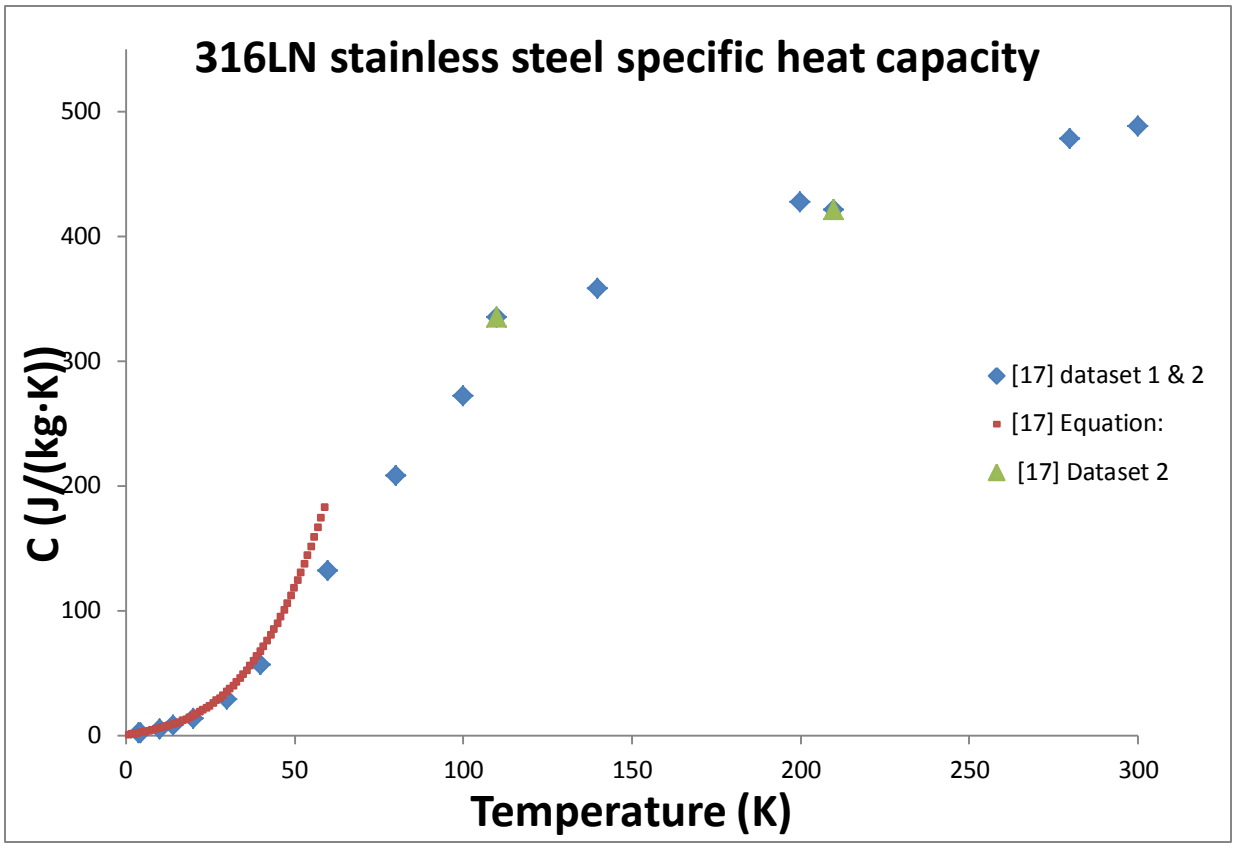
316LN stainless steel specific heat capacity
C (J/(kg·K))
Temperature (K)
[17] dataset 1 & 2
[17] Equation:
[17] Dataset 2
0
100
200
300
400
500
0
50
100
150
200
250
300

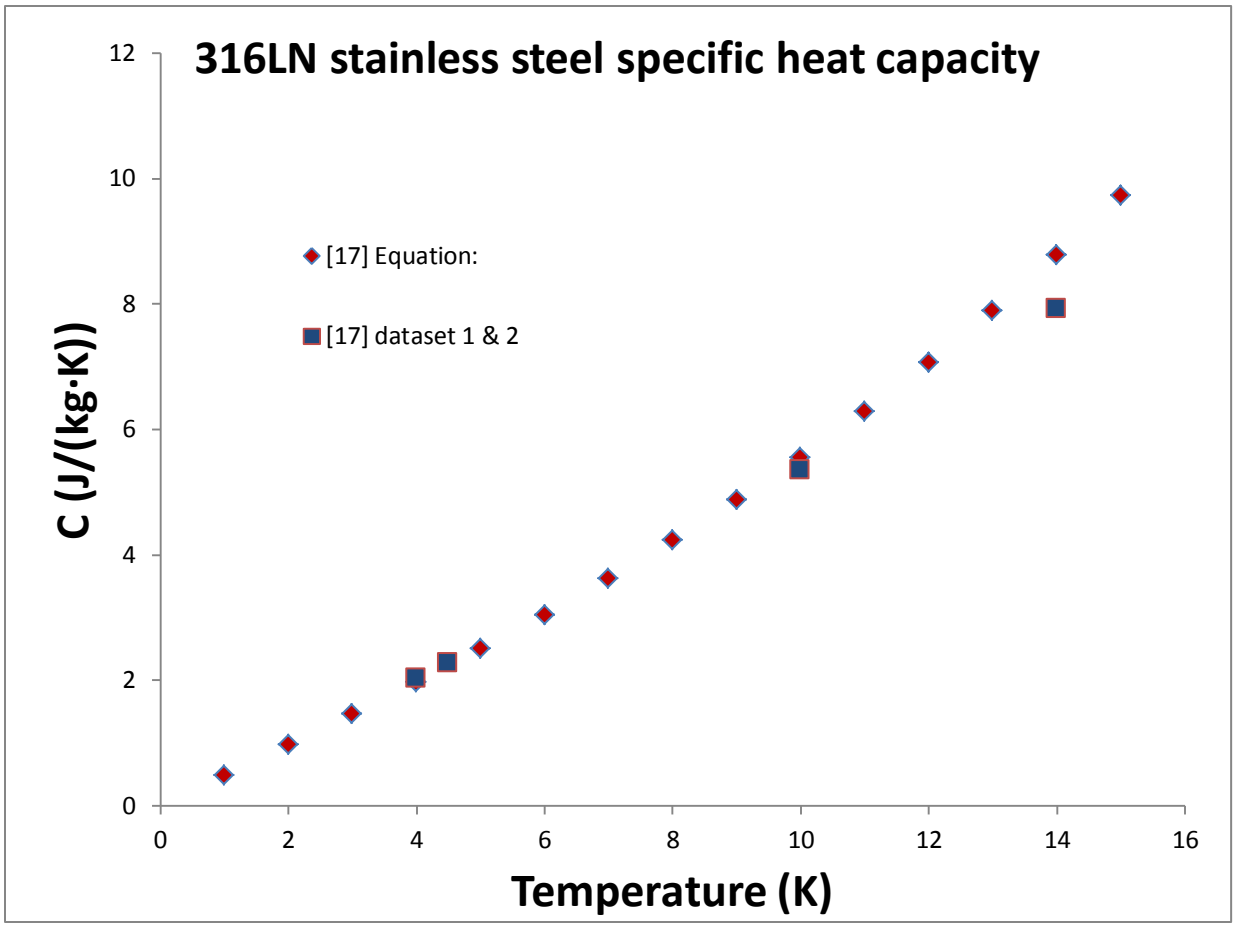
316LN stainless steel specific heat capacity
C (J/(kg·K))
Temperature (K)
[17] Equation:
[17] dataset 1 & 2
0
2
4
6
8
10
12
0
2
4
6
8
10
12
14
16

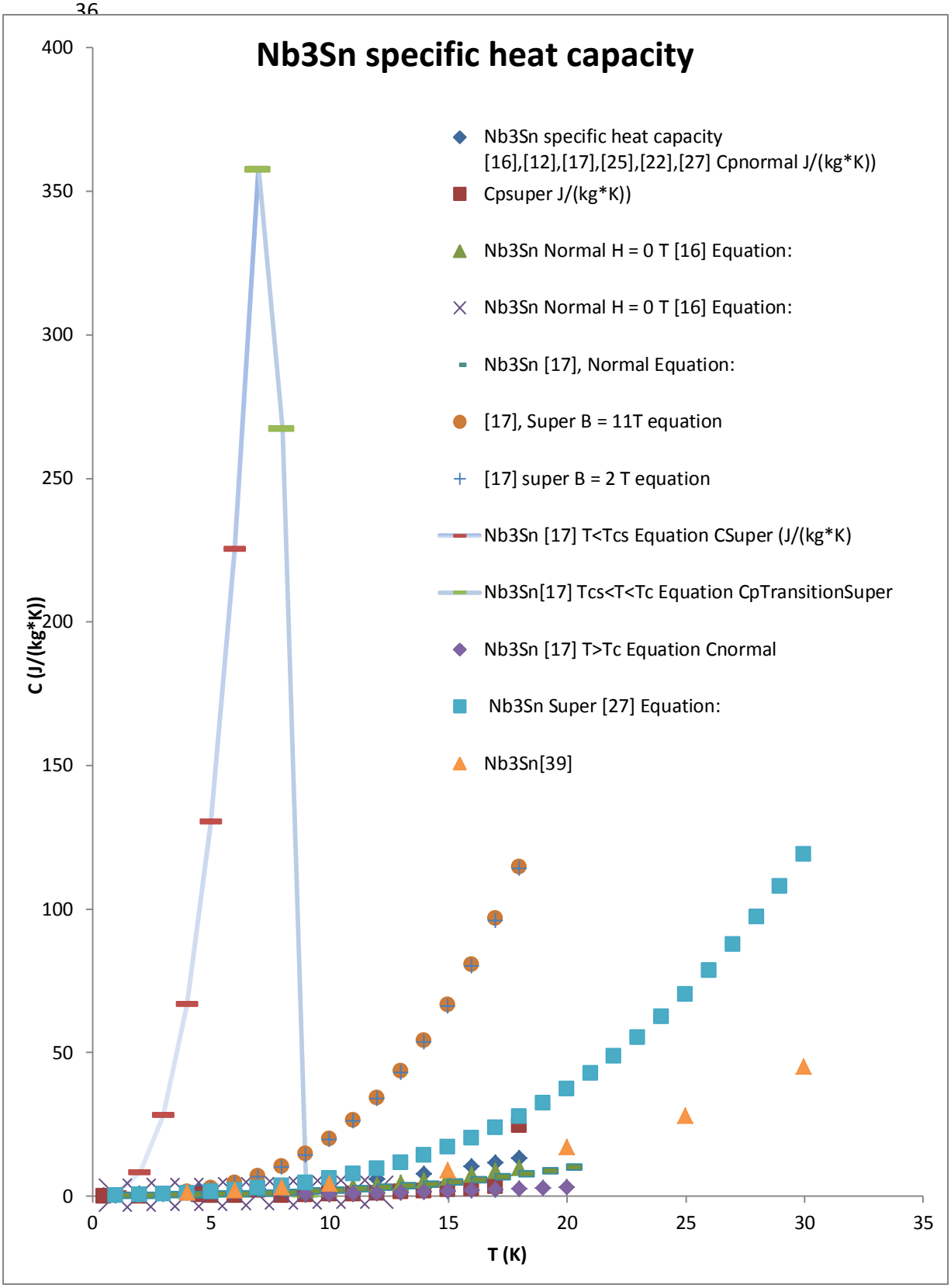
Nb3Sn specific heat capacity
Nb3Sn specific heat capacity [16],[12],[17],[25],[22],[27] Cpnormal J/(kg*K))
Cpsuper J/(kg*K))
Nb3Sn Normal H = 0 T [16] Equation:
Nb3Sn Normal H = 0 T [16] Equation:
Nb3Sn [17], Normal Equation:
[17], Super B = 11T equation
[17] super B = 2 T equation
Nb3Sn [17] T<Tcs Equation CSuper (J/(kg*K)
Nb3Sn[17] Tcs<T<Tc Equation CpTransitionSuper
Nb3Sn [17] T>Tc Equation Cnormal
Nb3Sn Super [27] Equation:
Nb3Sn[39]
C (J/(kg*K))
T (K)
0
50
100
150
200
250
300
350
400
0
5
10
15
20
25
30
35

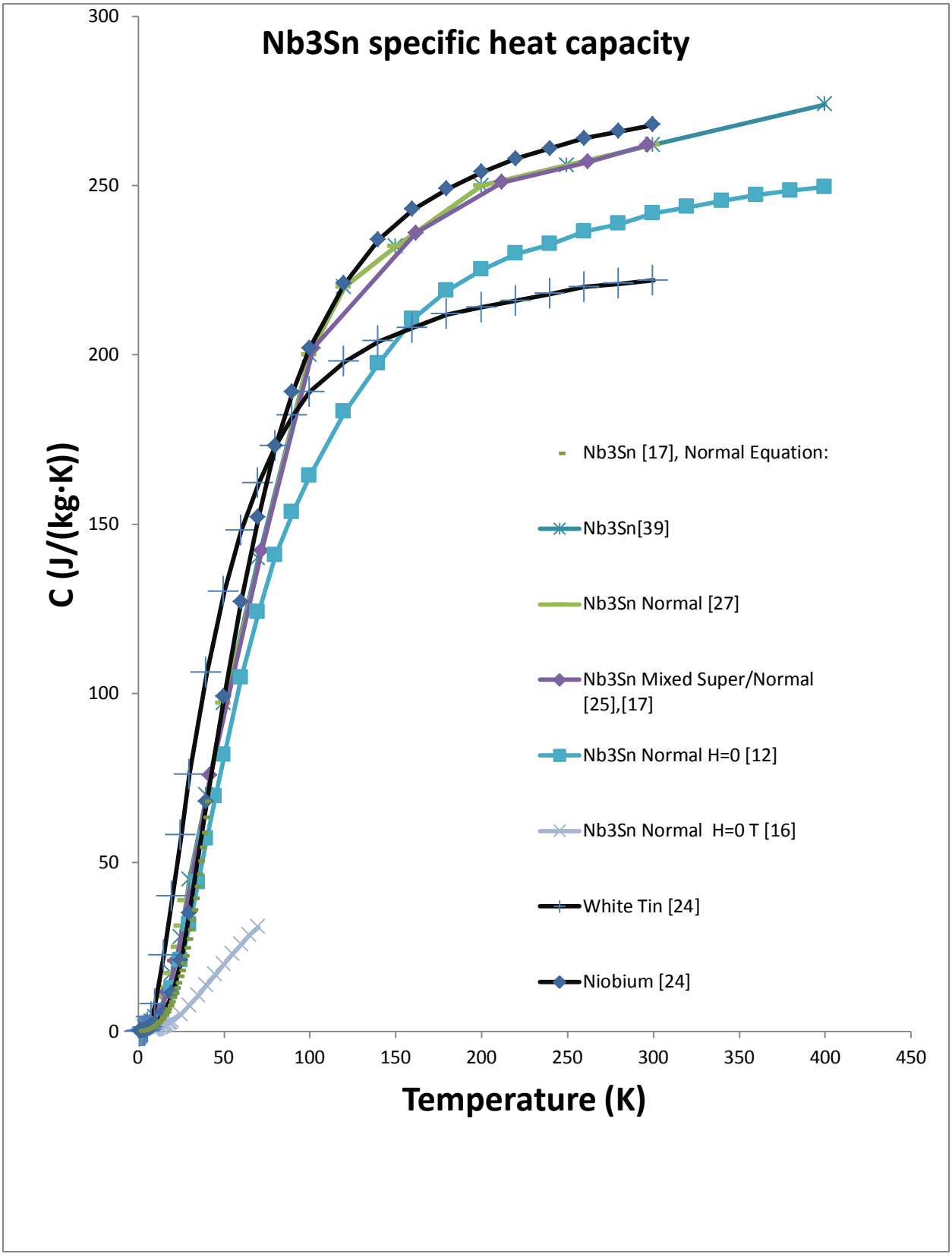
Nb3Sn specific heat capacity
C (J/(kg·K))
Temperature (K)
0
50
100
150
200
250
300
350
400
450
Nb3Sn [17], Normal Equation:
Nb3Sn[39]
Nb3Sn Normal [27]
Nb3Sn Mixed Super/Normal [25],[17]
Nb3Sn Normal H=0 [12]
Nb3Sn Normal H=0 T [16]
White Tin [24]
Niobium [24]

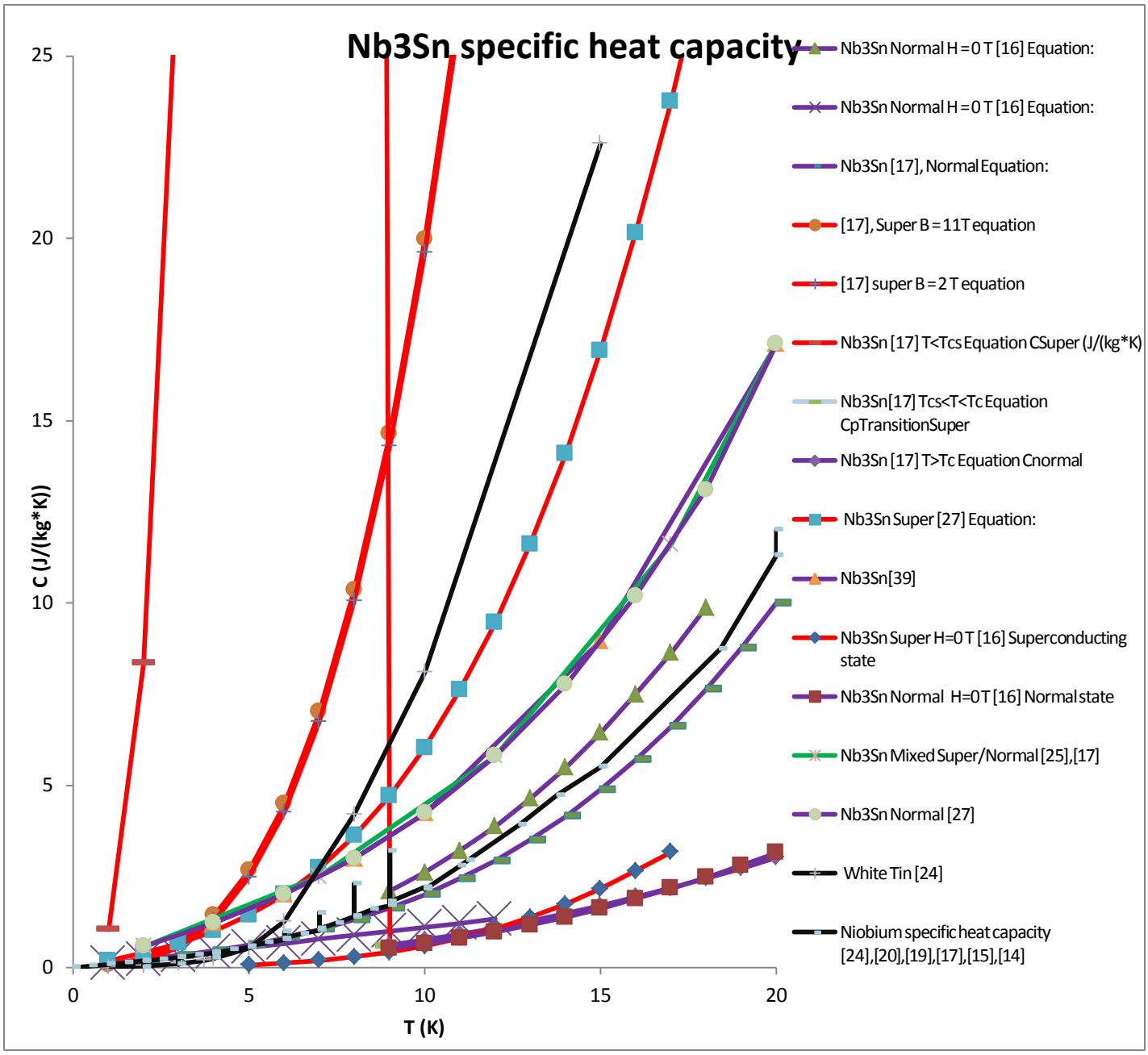
Nb3Sn specific heat capacity
C (J/(kg*K))
T (K)
0
5
10
15
20
25
Nb3Sn Normal H = 0 T [16] Equation:
Nb3Sn Normal H = 0 T [16] Equation:
Nb3Sn [17], Normal Equation:
[17], Super B = 11T equation
[17] super B = 2 T equation
Nb3Sn [17] T<Tcs Equation CSuper (J/(kg*K)
Nb3Sn[17] Tcs<T<Tc Equation CpTransitionSuper
Nb3Sn [17] T>Tc Equation Cnormal
Nb3Sn Super [27] Equation:
Nb3Sn[39]
Nb3Sn Super H=0 T [16] Superconducting state
Nb3Sn Normal H=0 T [16] Normal state
Nb3Sn Mixed Super/Normal [25],[17]
Nb3Sn Normal [27]
White Tin [24]
Niobium specific heat capacity [24],[20],[19],[17],[15],[14]

Figure 1: [23] Nb3Sn magnetic field data, a 2nd order phase transition to superconducting shifts with changing magnetic field.

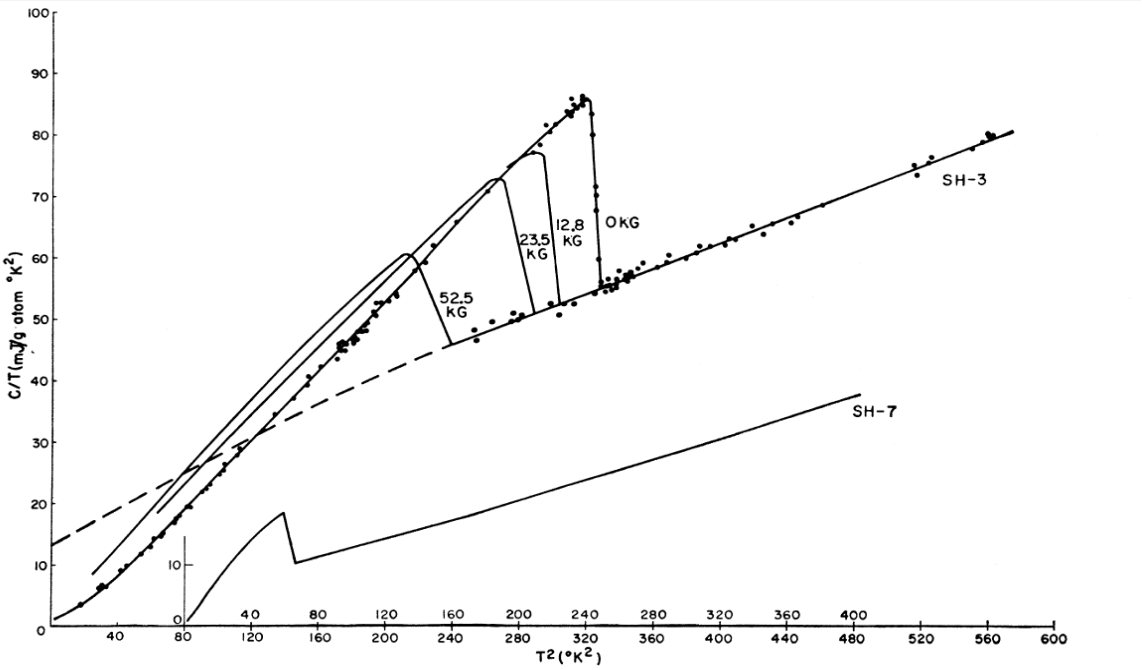

FIG. 3. Specific heat of Nb_3Sn (sample *SH*-3) in various fields, and Nb_4Sn (sample *SH*-7) at zero field. The vertical scale is the same for both samples, as is the gram-atomic volume, 11.1 cm³. The dashed line is the normal-state behavior of Nb_3Sn inferred by analogy to the behavior of Hg (see text).

Figure 2: [23} softening of the 2nd order peak due to imperfect composition.

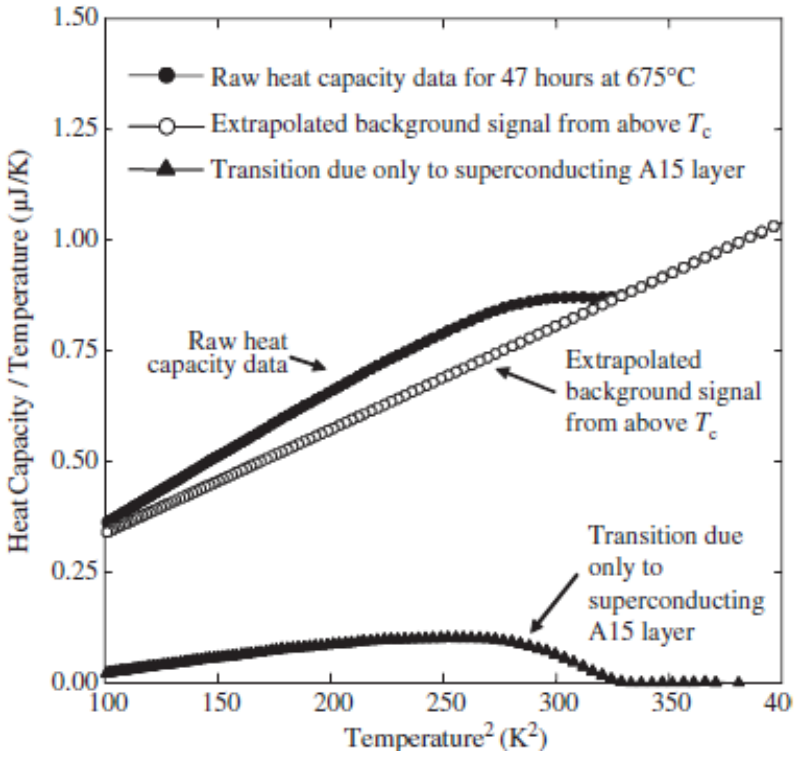

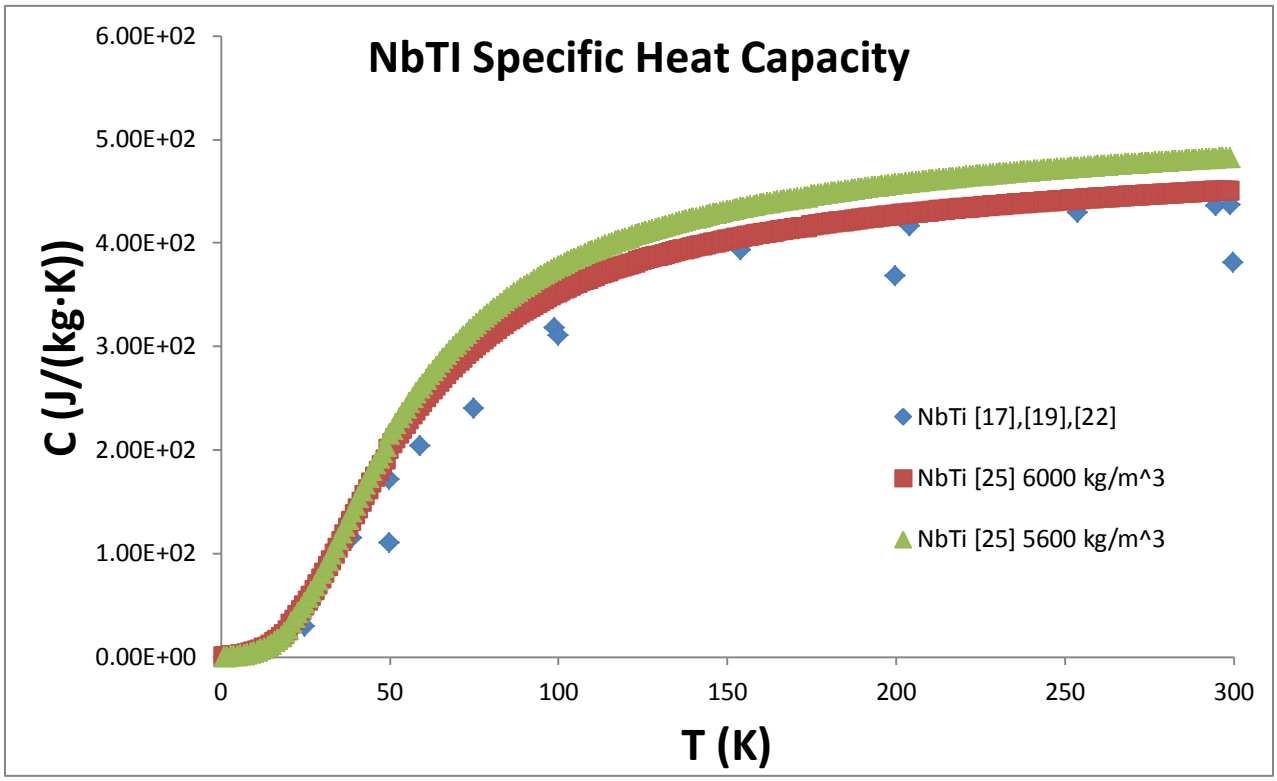
NbTI Specific Heat Capacity
C (J/(kg·K))
T (K)
6.00E+02
5.00E+02
4.00E+02
3.00E+02
2.00E+02
1.00E+02
0.00E+00
0
50
100
150
200
250
300
NbTi [17],[19],[22]
NbTi [25] 6000 kg/m^3
NbTi [25] 5600 kg/m^3

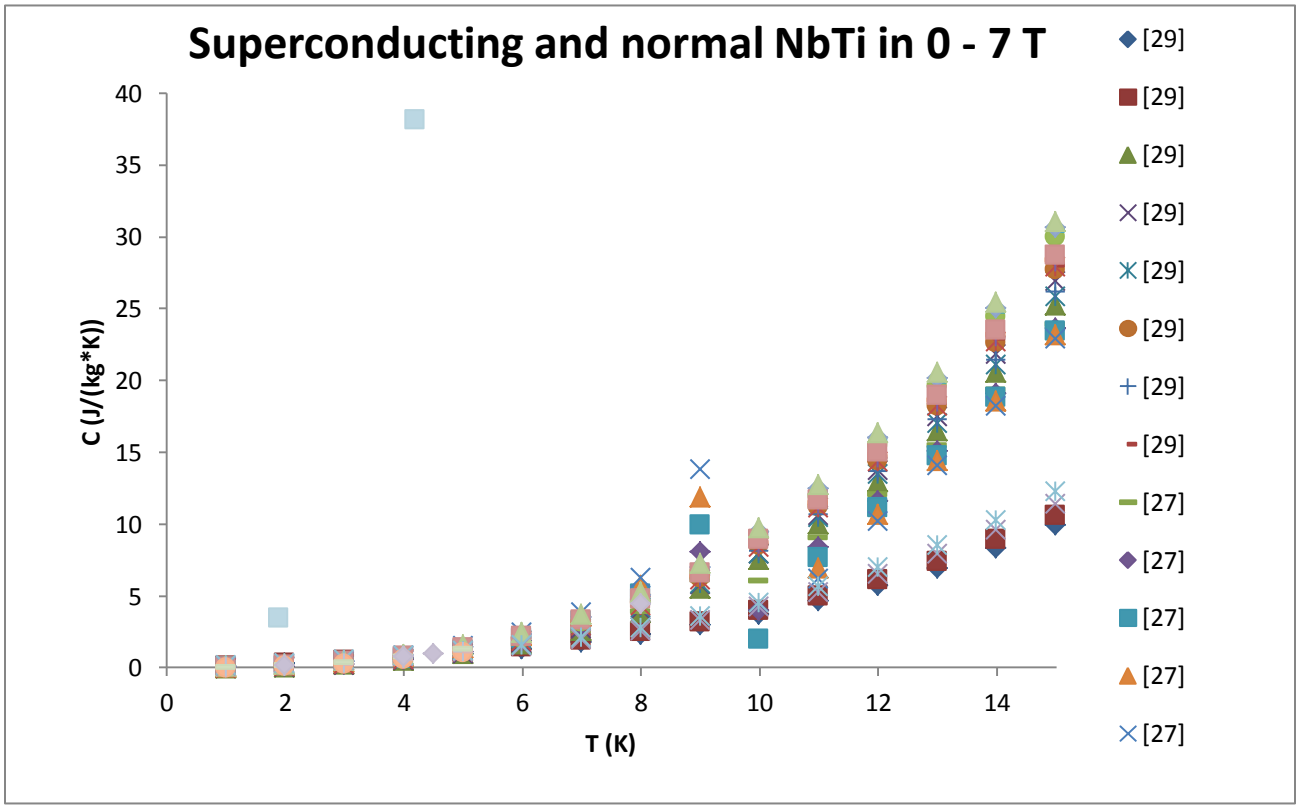
Superconducting and normal NbTi in 0 - 7 T
C (J/(kg*K))
T (K)
40
35
30
25
20
15
10
5
0
0
2
4
6
8
10
12
14
[29]
[29]
[29]
[29]
[29]
[29]
[29]
[27]
[27]
[27]
[27]
[27]

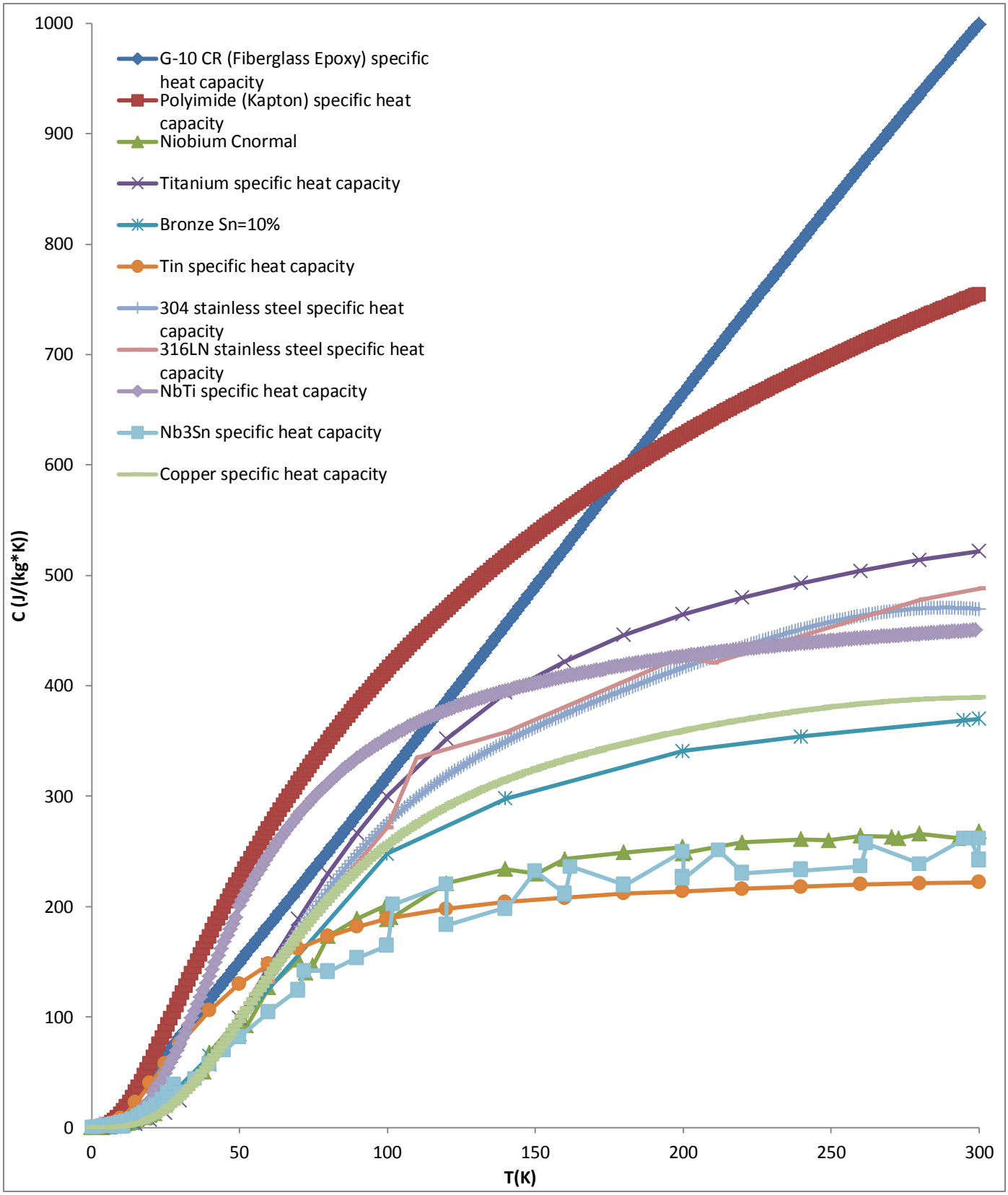
G-10 CR (Fiberglass Epoxy) specific heat capacity
Polyimide (Kapton) specific heat capacity
Niobium Cnormal
Titanium specific heat capacity
Bronze Sn=10%
Tin specific heat capacity
304 stainless steel specific heat capacity
316LN stainless steel specific heat capacity
NbTi specific heat capacity
Nb3Sn specific heat capacity
Copper specific heat capacity
C (J/(kg*K))
T(K)
0
100
200
300
400
500
600
700
800
900
1000
0
50
100
150
200
250
300

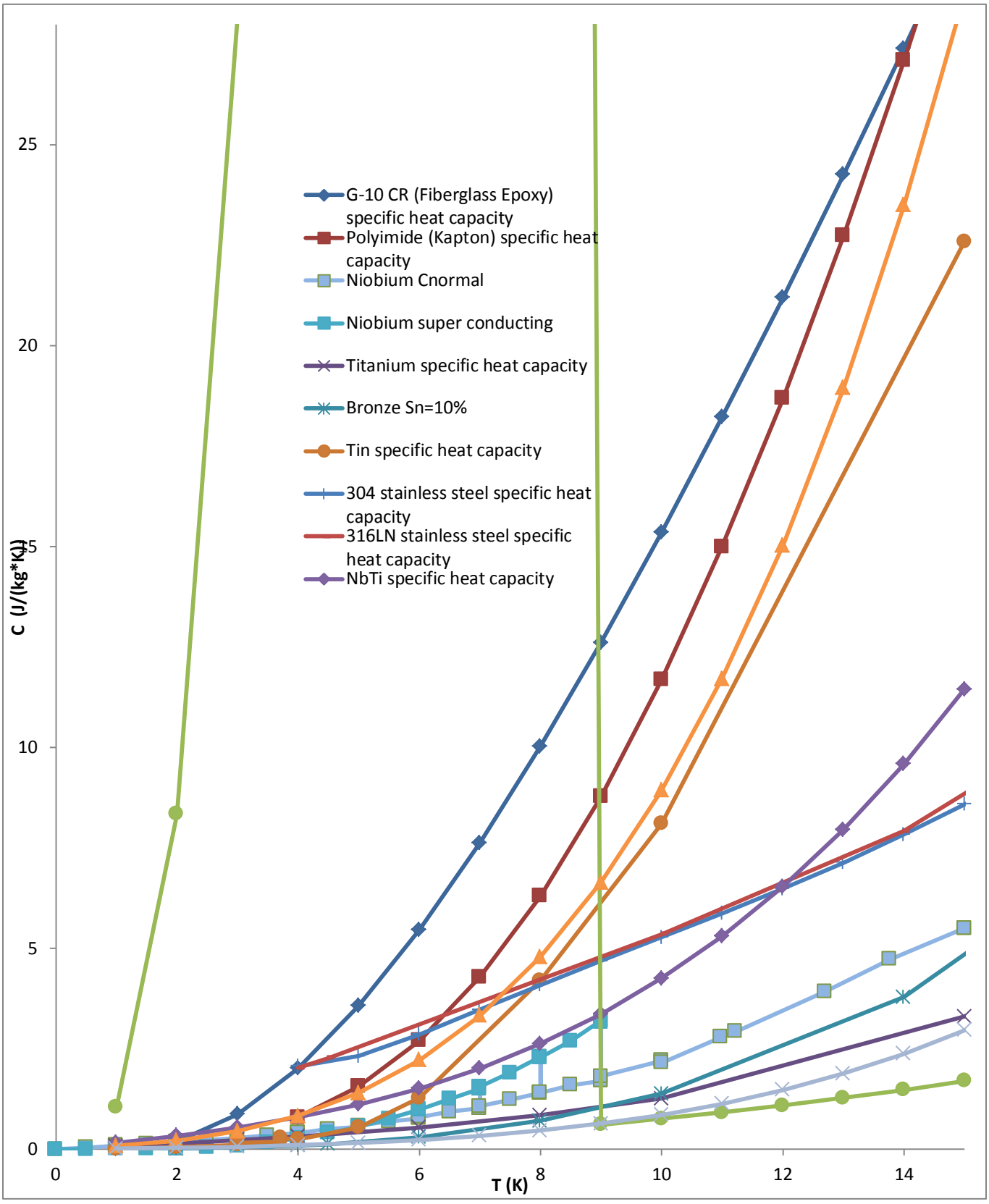
G-10 CR (Fiberglass Epoxy) specific heat capacity
Polyimide (Kapton) specific heat capacity
Niobium Cnormal
Niobium super conducting
Titanium specific heat capacity
Bronze Sn=10%
Tin specific heat capacity
304 stainless steel specific heat capacity
316LN stainless steel specific heat capacity
NbTi specific heat capacity
C (J/(kg*K))
T (K)
0
5
10
15
20
25
0
2
4
6
8
10
12
14

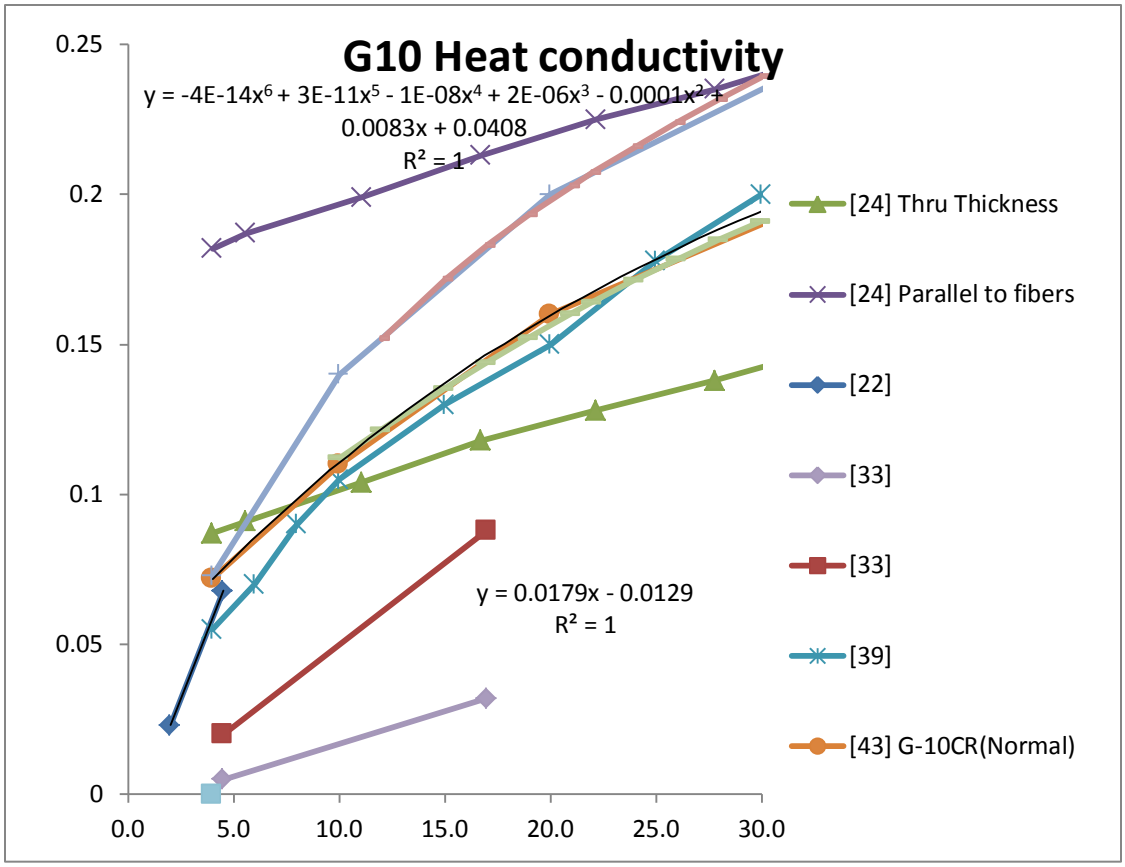
G10 Heat conductivity
y = -4E-14x⁶ + 3E-11x⁵ - 1E-08x⁴ + 2E-06x³ - 0.0001x² + 0.0083x + 0.0408
R² = 1
y = 0.0179x - 0.0129
R² = 1
0.25
0.2
0.15
0.1
0.05
0
0.0
5.0
10.0
15.0
20.0
25.0
30.0
[24] Thru Thickness
[24] Parallel to fibers
[22]
[33]
[33]
[39]
[43] G-10CR(Normal)

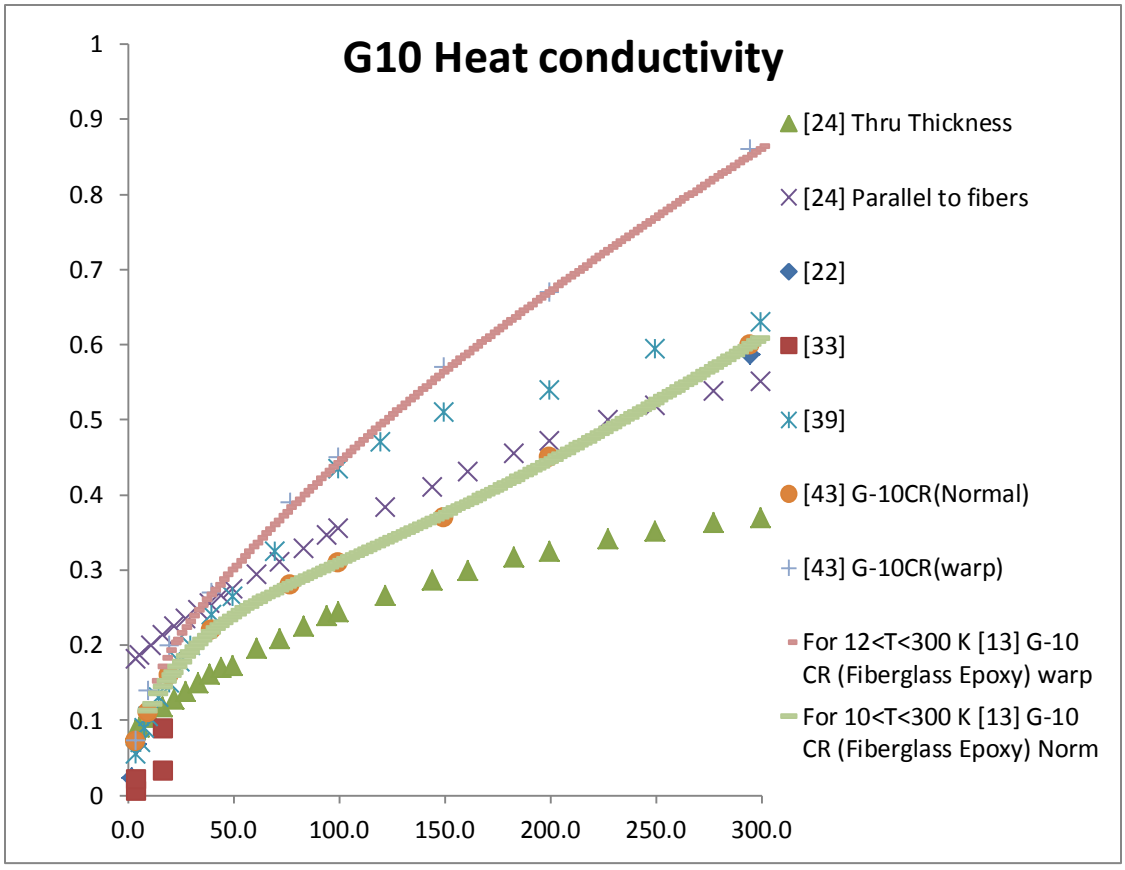
G10 Heat conductivity
1
0.9
0.8
0.7
0.6
0.5
0.4
0.3
0.2
0.1
0
0.0
50.0
100.0
150.0
200.0
250.0
300.0
[24] Thru Thickness
[24] Parallel to fibers
[22]
[33]
[39]
[43] G-10CR(Normal)
[43] G-10CR(warp)
For 12<T<300 K [13] G-10 CR (Fiberglass Epoxy) warp
For 10<T<300 K [13] G-10 CR (Fiberglass Epoxy) Norm

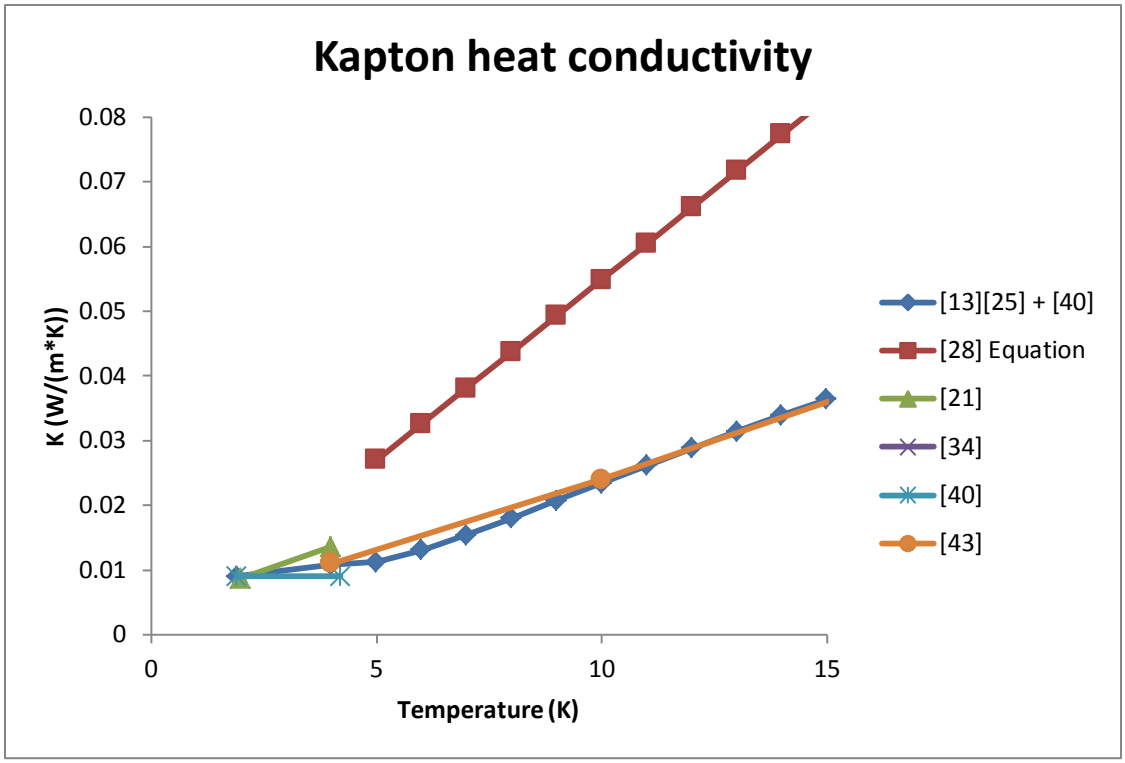
Kapton heat conductivity
K (W/(m*K))
0.08
0.07
0.06
0.05
0.04
0.03
0.02
0.01
0
0
5
10
15
Temperature (K)
[13][25] + [40]
[28] Equation
[21]
[34]
[40]
[43]

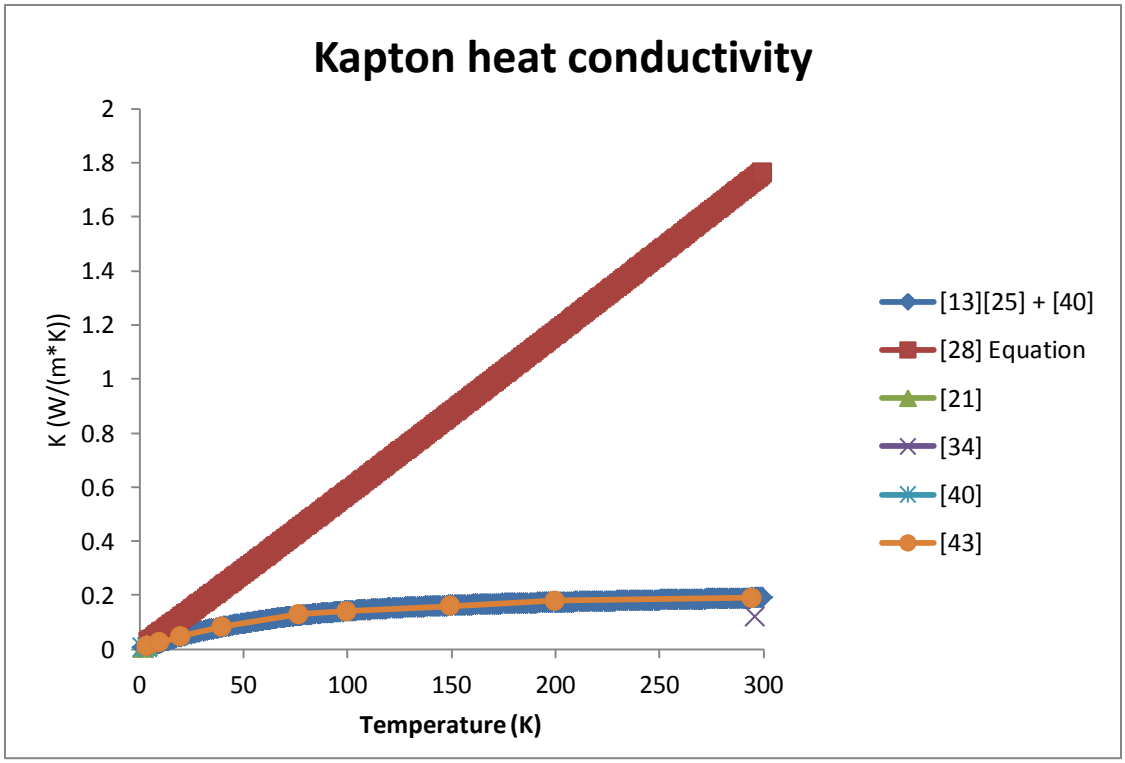
Kapton heat conductivity
K (W/(m*K))
2
1.8
1.6
1.4
1.2
1
0.8
0.6
0.4
0.2
0
0
50
100
150
200
250
300
Temperature (K)
[13][25] + [40]
[28] Equation
[21]
[34]
[40]
[43]

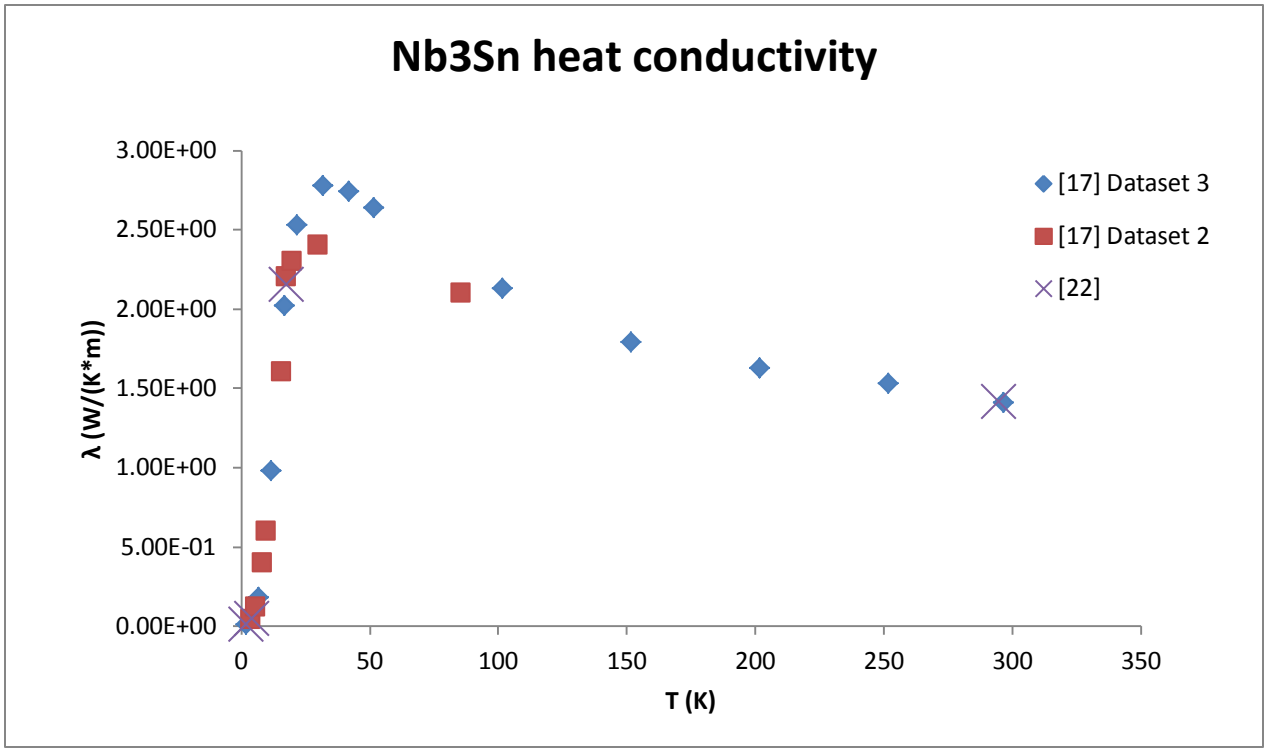
Nb3Sn heat conductivity
3.00E+00
2.50E+00
2.00E+00
1.50E+00
1.00E+00
5.00E-01
0.00E+00
λ (W/(K*m))
0
50
100
150
200
250
300
350
T (K)
[17] Dataset 3
[17] Dataset 2
[22]

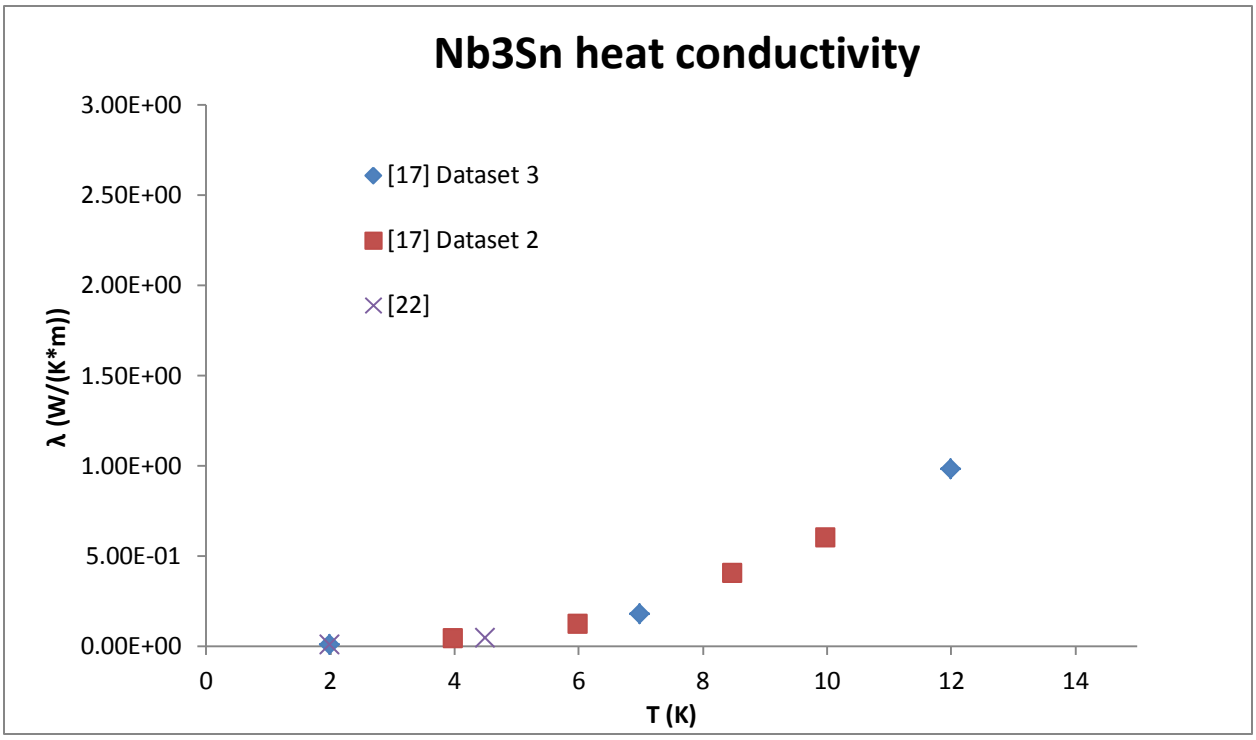
Nb3Sn heat conductivity
3.00E+00
2.50E+00
2.00E+00
1.50E+00
1.00E+00
5.00E-01
0.00E+00
λ (W/(K*m))
0
2
4
6
8
10
12
14
T (K)
[17] Dataset 3
[17] Dataset 2
[22]

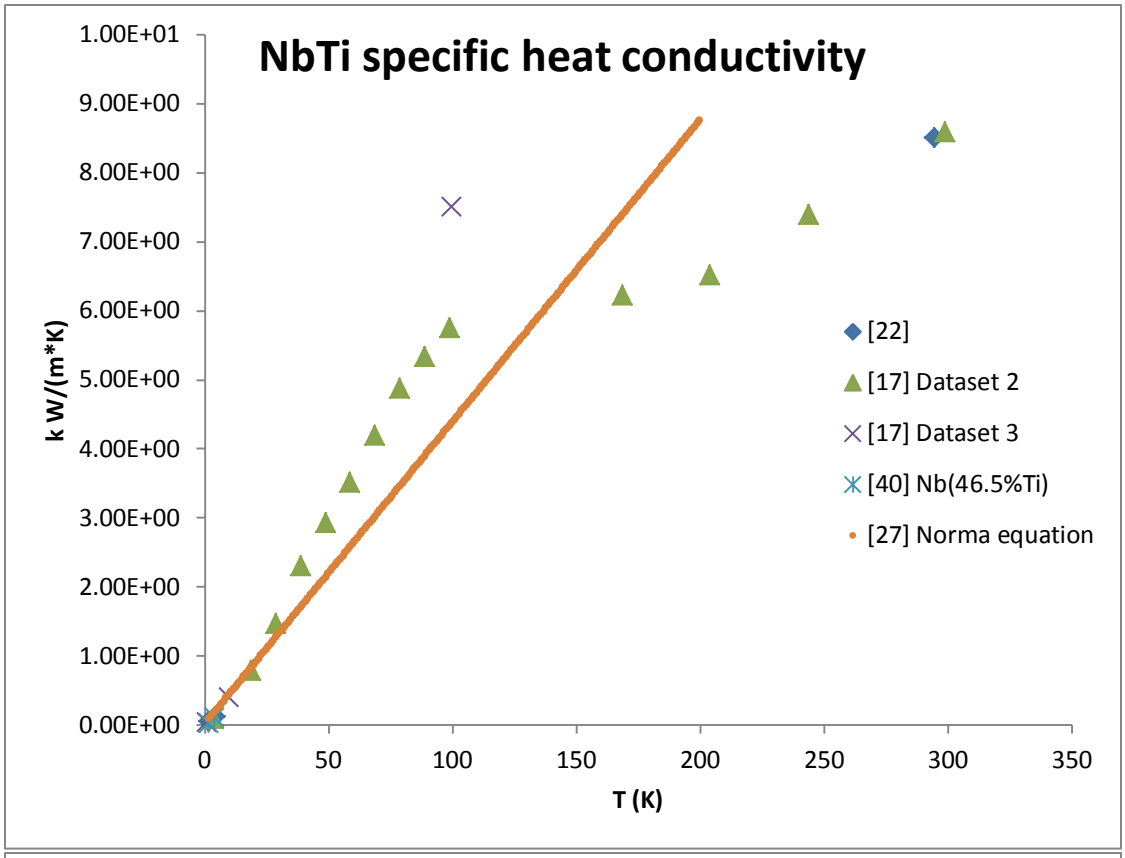
NbTi specific heat conductivity
k W/(m*K)
T (K)
1.00E+01
9.00E+00
8.00E+00
7.00E+00
6.00E+00
5.00E+00
4.00E+00
3.00E+00
2.00E+00
1.00E+00
0.00E+00
0
50
100
150
200
250
300
350
[22]
[17] Dataset 2
[17] Dataset 3
[40] Nb(46.5%Ti)
[27] Norma equation

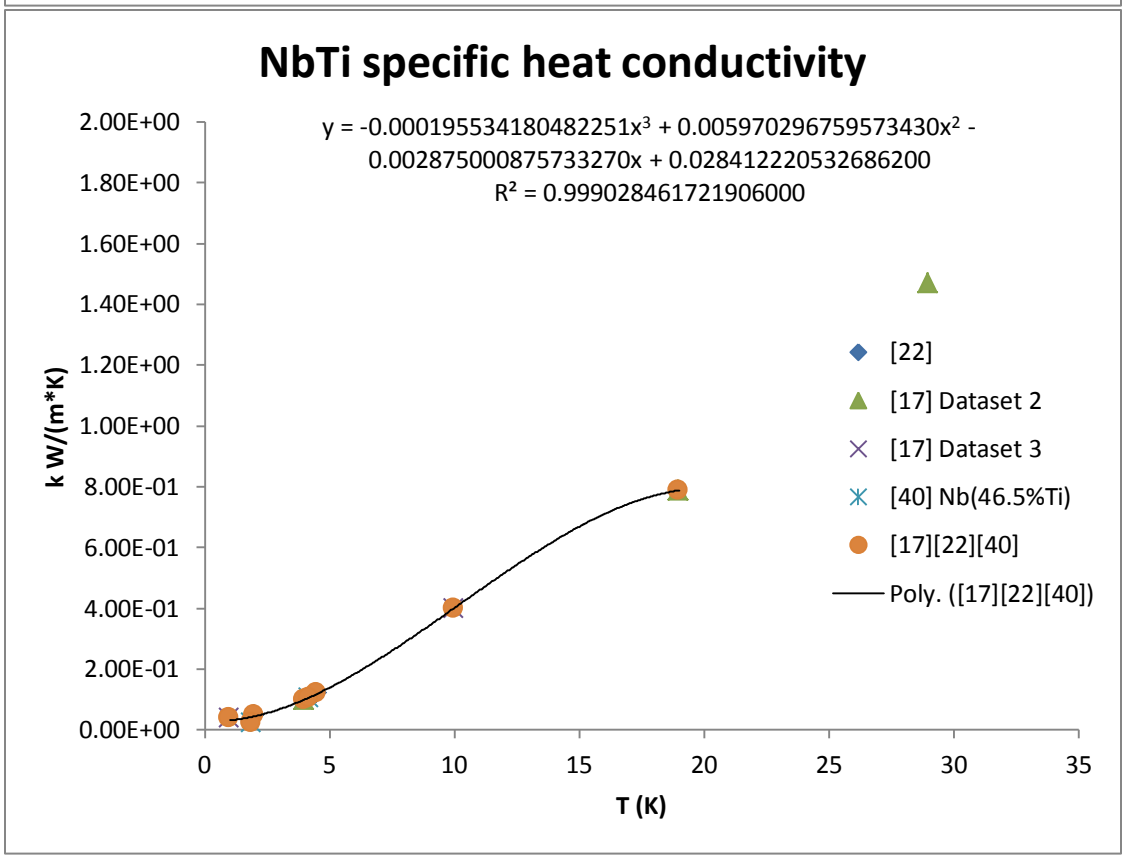
NbTi specific heat conductivity
y = -0.00019553418048225 1x³ + 0.005970296759573430x² - 0.002875000875733270x + 0.028412220532686200
R² = 0.999028461721906000
k W/(m*K)
T (K)
2.00E+00
1.80E+00
1.60E+00
1.40E+00
1.20E+00
1.00E+00
8.00E-01
6.00E-01
4.00E-01
2.00E-01
0.00E+00
0
5
10
15
20
25
30
35
[22]
[17] Dataset 2
[17] Dataset 3
[40] Nb(46.5%Ti)
[17][22][40]
Poly. ([17][22][40])

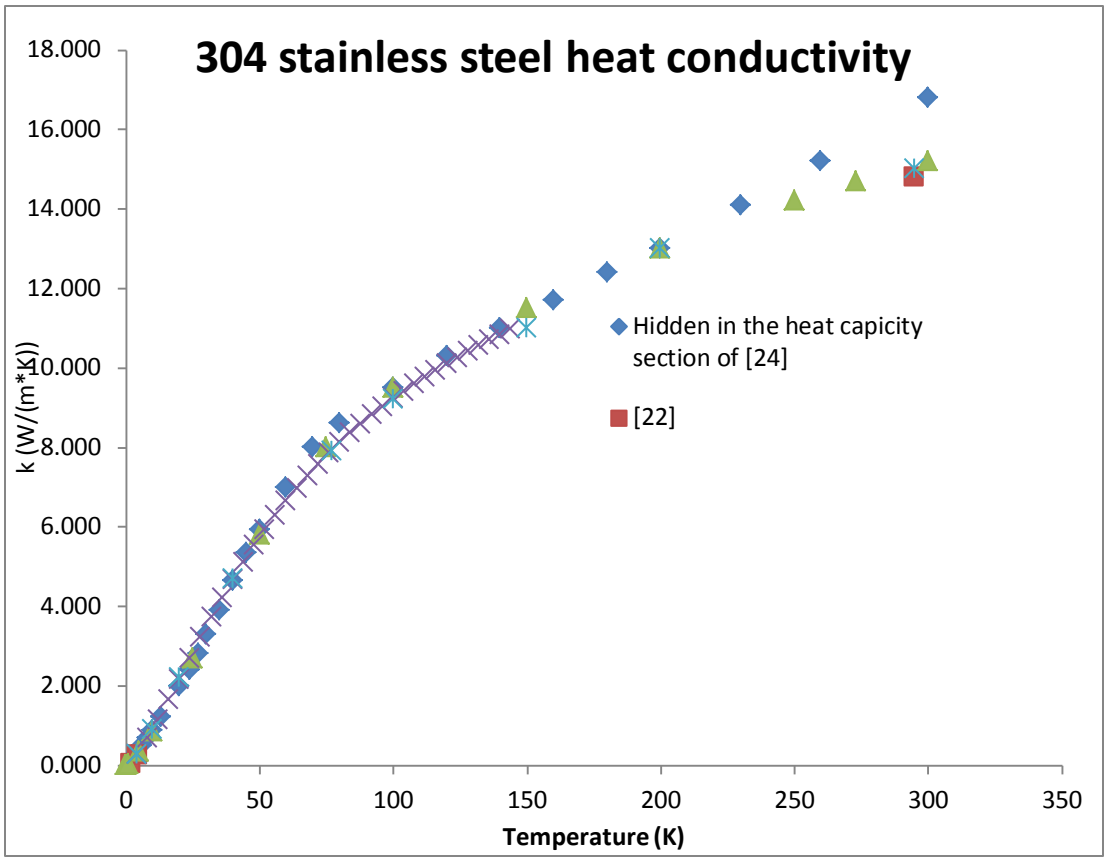
304 stainless steel heat conductivity
18.000
16.000
14.000
12.000
10.000
8.000
6.000
4.000
2.000
0.000
k (W/(m*K))
0
50
100
150
200
250
300
350
Temperature (K)
Hidden in the heat capicity section of [24]
[22]

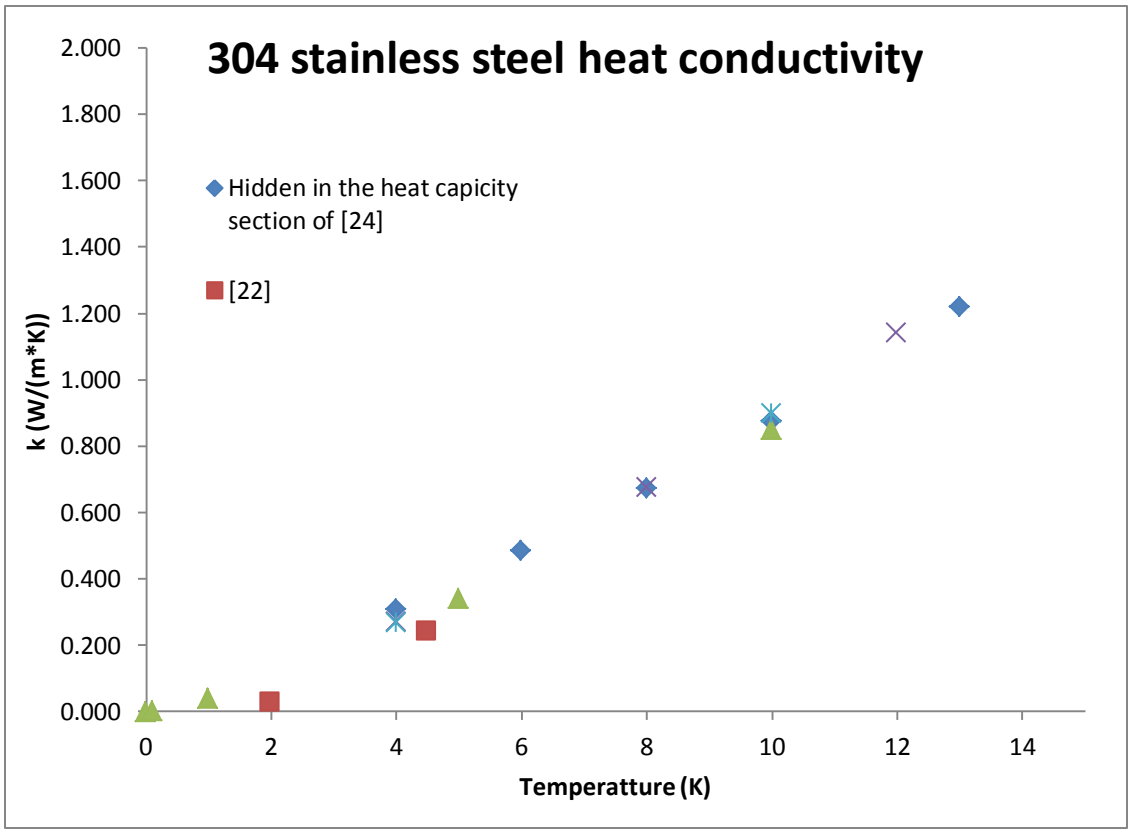
304 stainless steel heat conductivity
2.000
1.800
1.600
1.400
1.200
1.000
0.800
0.600
0.400
0.200
0.000
k (W/(m*K))
0
2
4
6
8
10
12
14
Temperatture (K)
Hidden in the heat capicity section of [24]
[22]

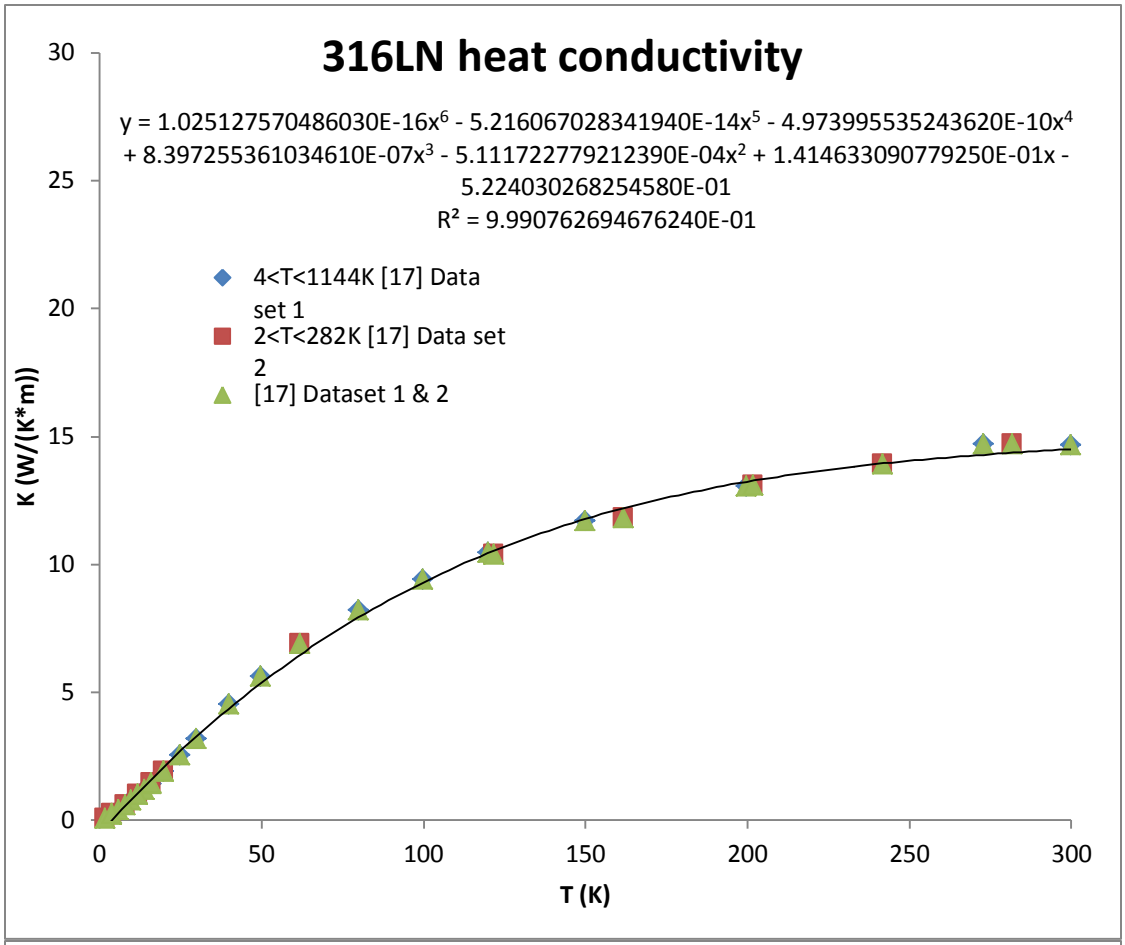
316LN heat conductivity
y = 1.025127570486030E-16x^6 - 5.216067028341940E-14x^5 - 4.973995535243620E-10x^4 + 8.397255361034610E-07x^3 - 5.111722779212390E-04x^2 + 1.414633090779250E-01x - 5.224030268254580E-01
R² = 9.990762694676240E-01
4<T<1144K [17] Data set 1
2<T<282K [17] Data set 2
[17] Dataset 1 & 2
K (W/(K*m))
T (K)
0
5
10
15
20
25
30
0
50
100
150
200
250
300

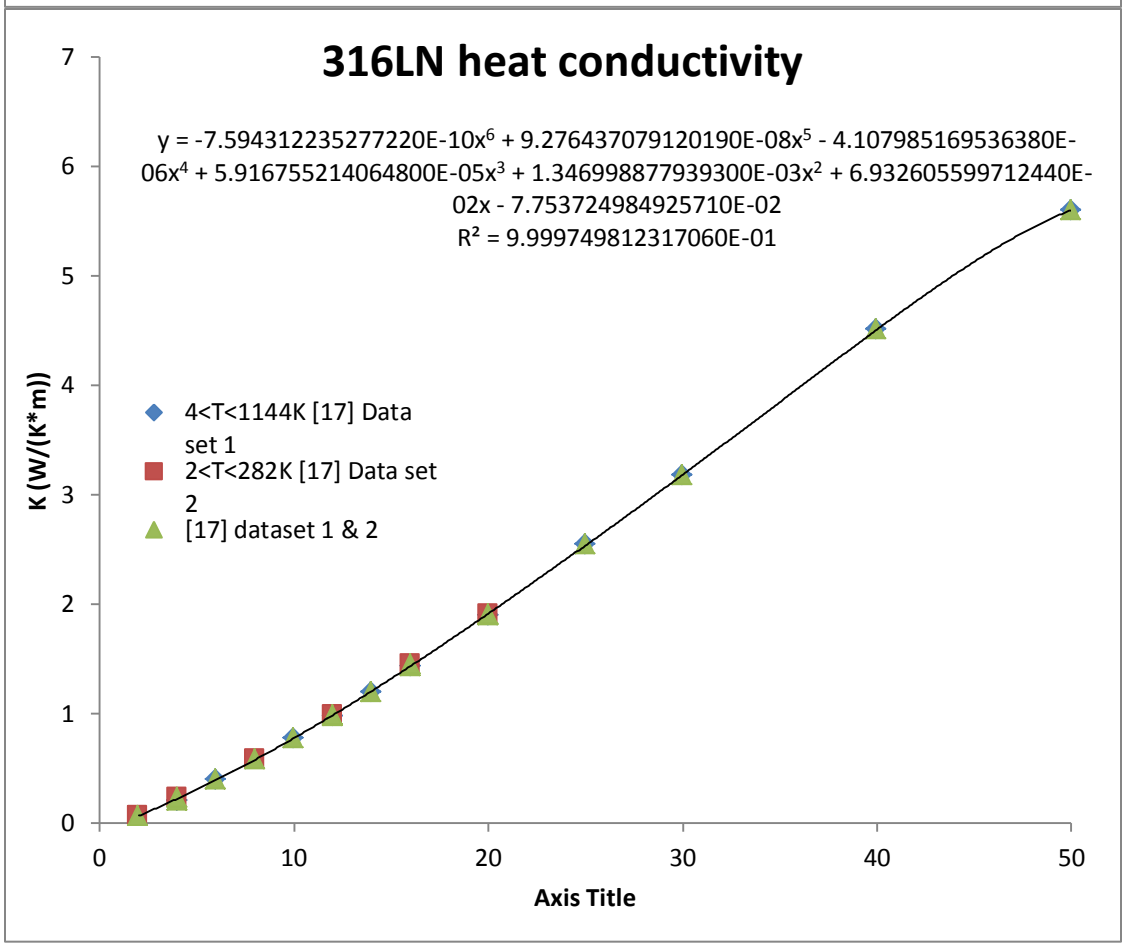
316LN heat conductivity
y = -7.594312235277220E-10x^6 + 9.276437079120190E-08x^5 - 4.107985169536380E-06x^4 + 5.916755214064800E-05x^3 + 1.346998877939300E-03x^2 + 6.932605599712440E-02x - 7.753724984925710E-02
R² = 9.999749812317060E-01
4<T<1144K [17] Data set 1
2<T<282K [17] Data set 2
[17] dataset 1 & 2
K (W/(K*m))
Axis Title
0
1
2
3
4
5
6
7
0
10
20
30
40
50

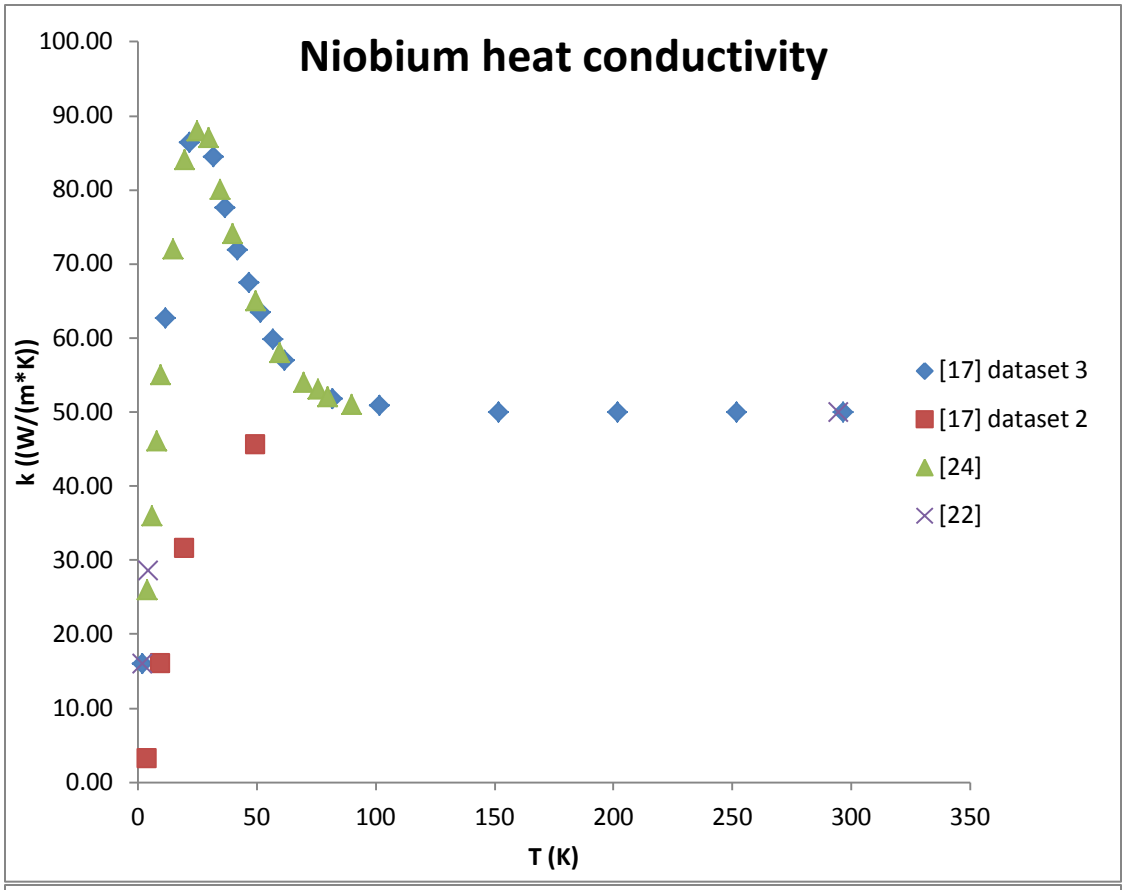
Niobium heat conductivity
k ((W/(m*K))
T (K)
100.00
90.00
80.00
70.00
60.00
50.00
40.00
30.00
20.00
10.00
0.00
0
50
100
150
200
250
300
350
[17] dataset 3
[17] dataset 2
[24]
[22]

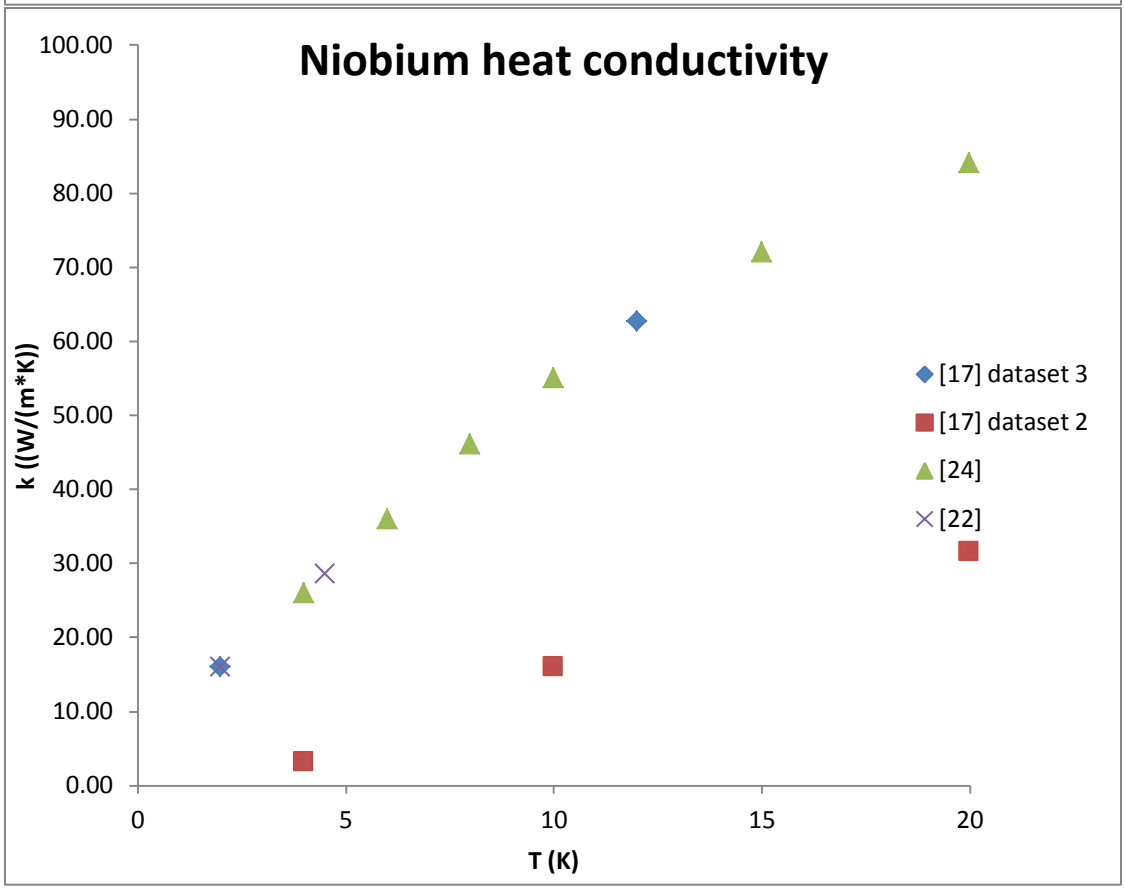
Niobium heat conductivity
k ((W/(m*K))
T (K)
100.00
90.00
80.00
70.00
60.00
50.00
40.00
30.00
20.00
10.00
0.00
0
5
10
15
20
[17] dataset 3
[17] dataset 2
[24]
[22]

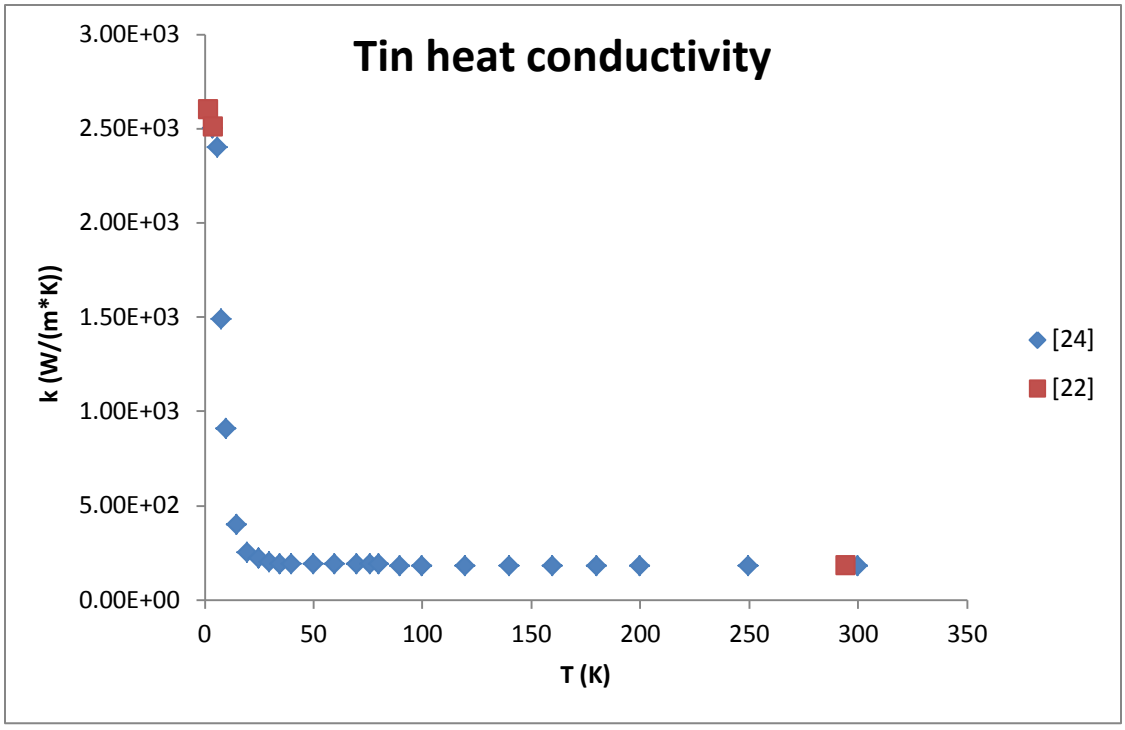
Tin heat conductivity
3.00E+03
2.50E+03
2.00E+03
1.50E+03
1.00E+03
5.00E+02
0.00E+00
k (W/(m*K))
0
50
100
150
200
250
300
350
T (K)
[24]
[22]

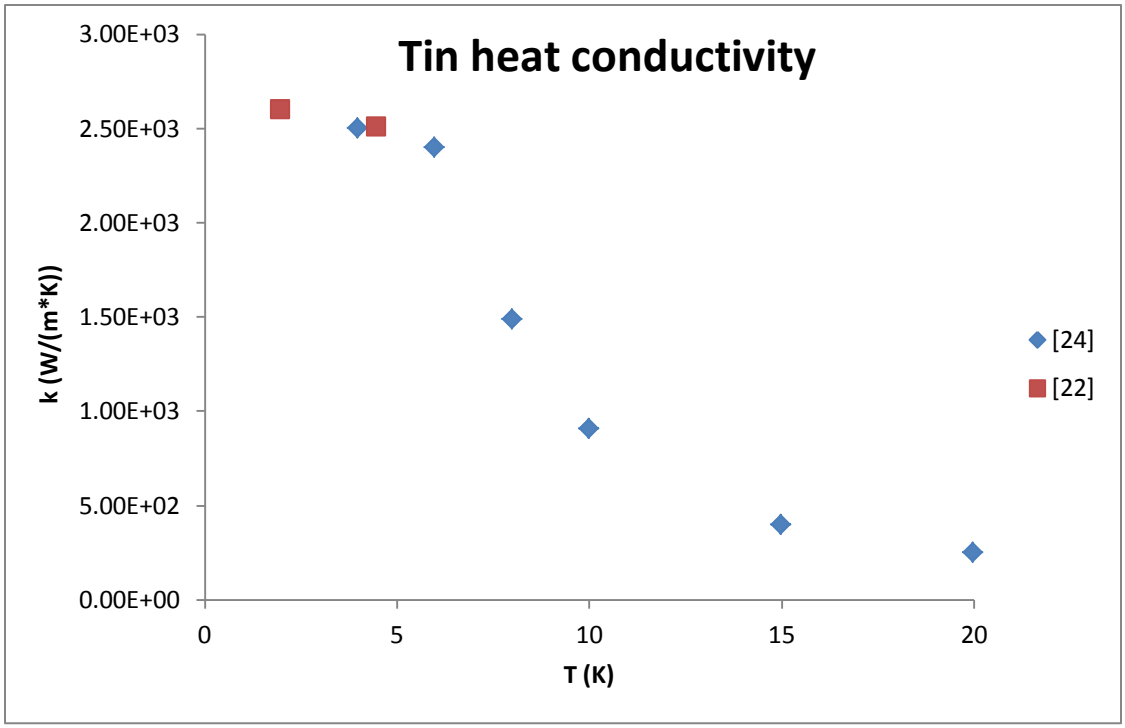
Tin heat conductivity
3.00E+03
2.50E+03
2.00E+03
1.50E+03
1.00E+03
5.00E+02
0.00E+00
k (W/(m*K))
0
5
10
15
20
T (K)
[24]
[22]

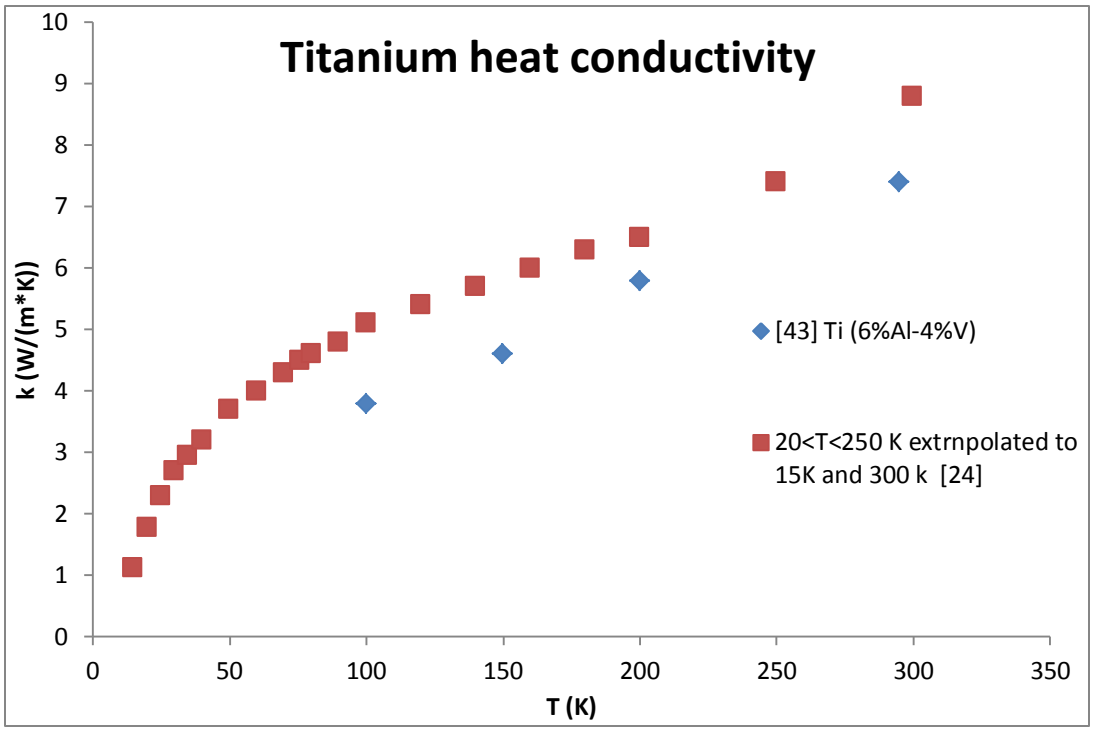
Titanium heat conductivity
k (W/(m*K))
T (K)
[43] Ti (6%Al-4%V)
20<T<250 K extrnpolated to 15K and 300 k [24]

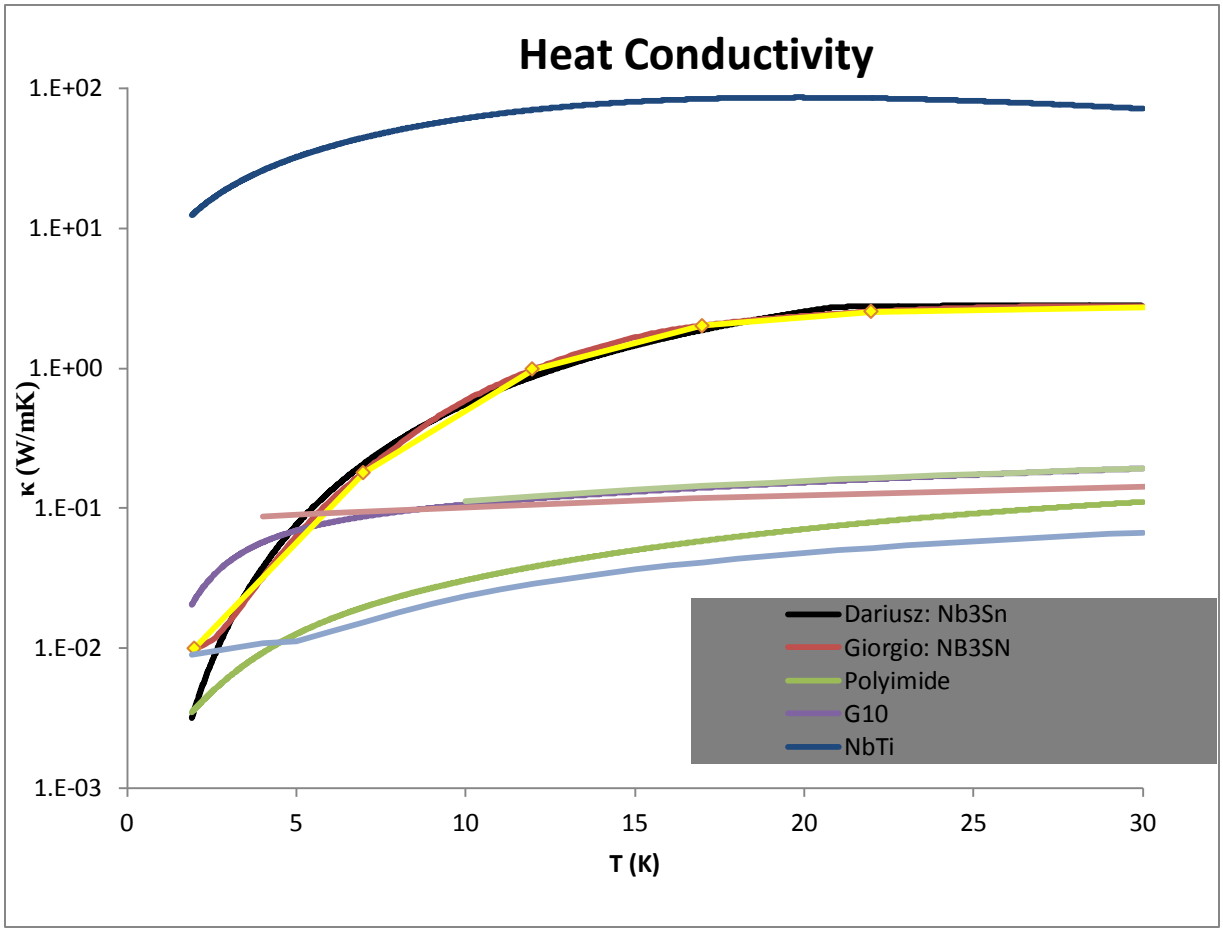
Heat Conductivity
κ (W/mK)
T (K)
Dariusz: Nb3Sn
Giorgio: NB3SN
Polyimide
G10
NbTi

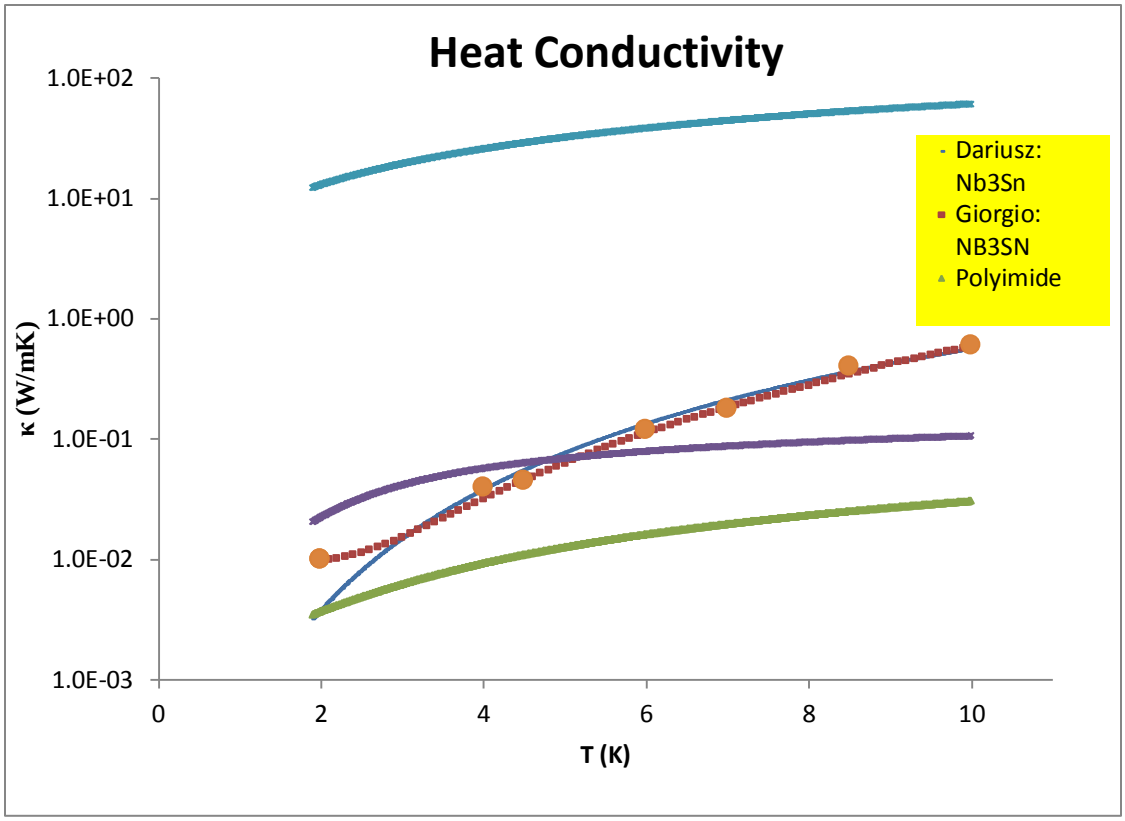
Heat Conductivity
1.0E+02
1.0E+01
1.0E+00
1.0E-01
1.0E-02
1.0E-03
κ (W/mK)
0
2
4
6
8
10
T (K)
Dariusz: Nb3Sn
Giorgio: NB3SN
Polyimide

4.2 Appendix 2

Table 3: Density of materials

G10		Epoxy		Polyimide		Copper		Titanium		Bronze	
ρ (kg/m^3)	Ref	ρ (kg/m^3)	Ref	ρ (kg/m^3)	Ref	ρ (kg/m^3)	Ref	ρ (kg/m^3)	Ref	ρ (kg/m^3)	Ref
1900	[22]	1800	[30]	1420	[34]	8960	[39]	4540	[22]	8850	[22]
1900	[30]	300	[40]	1417	[35]					8850	[17]
1948	[39]			1420	[40]					8960	[39]

Tin		Niobium		NbTi		Nb3Sn		316LN		304 SS	
ρ (kg/m^3)	Ref	ρ (kg/m^3)	Ref	ρ (kg/m^3)	Ref	ρ (kg/m^3)	Ref	ρ (kg/m^3)	Ref	ρ (kg/m^3)	Ref
7290	[22]	8570	[22]	5600	[22]	5400	[22]	7900	[17]	7080	[22]
		8600	[41]	6000	[27]	5400	[27]				
T (K)	ρ (kg/m^3) [24]			6000	[17]	8040	[30]			T (K)	ρ (kg/m^3) [24]
0	7418	T(K)	ρ (kg/m^3) [24]	6020	[40]	8040	[17]			0	7998
100	7375	0	8610			5400	[39]			100	7967
200	7331	100	8600							200	7934
286.36	7290	200	8590							300	7899
300	7283	300	8580								